Intragenic Recombination Influences Rotavirus Diversity and Evolution

Irene Hoxie[a,b] and John J. Dennehy[a,b,#]

[a]Biology Department, Queens College of The City University of New York, Queens, NY
[b]The Graduate Center of The City University of New York, New York, NY

Running head: Rotavirus Recombination and Evolution

#Address correspondence to John J. Dennehy, john.dennehy@qc.cuny.edu

Abstract

Because of their replication mode and segmented dsRNA genome, homologous recombination is assumed to be rare in the rotaviruses. We analyzed 23,627 complete rotavirus genome sequences available in the NCBI Virus Variation database, and found 109 instances of homologous recombination, at least 11 of which prevailed across multiple sequenced isolates. In one case, recombination may have generated a novel rotavirus VP1 lineage. We also found strong evidence for intergenotypic recombination in which more than one sequence strongly supported the same event, particularly between different genotypes of segment 9, which encodes the serotype protein, VP7. The recombined regions of many putative recombinants showed amino acid substitutions differentiating them from their major and minor parents. This finding suggests that these recombination events were not overly deleterious, since presumably these recombinants proliferated long enough to acquire adaptive mutations in their recombined regions. Protein structural predictions indicated that, despite the sometimes substantial amino acid replacements resulting from recombination, the overall protein structures remained relatively unaffected. Notably, recombination junctions appear to occur non-randomly with hot spots corresponding to secondary RNA structures, a pattern seen consistently across segments. In total, we found strong evidence for recombination in nine of eleven rotavirus A segments. Only segment 7 (NSP3) and segment 11 (NSP5) did not show strong evidence of recombination. Collectively, the results of our computational analyses suggest that, contrary to the prevailing sentiment, recombination may be a significant driver of rotavirus evolution and may influence circulating strain diversity.

Keywords: dsRNA, genetic diversity, *Reoviridae*, segmented genome, RDP4

Introduction

The non-enveloped, dsRNA rotaviruses of the family *Reoviridae* are a common cause of acute gastroenteritis in young individuals of many bird and mammal species (Desselberger 2014). The rotavirus genome consists of 11 segments, each coding for a single protein with the exception of segment 11, which encodes two proteins, NSP5 and NSP6 (Desselberger 2014). Six of the proteins are structural proteins (VP1-4, VP6 and VP7), and the remainder are non-structural proteins (NSP1-6). The infectious virion is a triple-layered particle consisting of two outer-layer proteins, VP4 and VP7, a middle layer protein, VP6, and an inner capsid protein, VP2. The RNA polymerase (VP1) and the capping-enzyme (VP3) are attached to the inner capsid protein. For the virus to be infectious (at least when not infecting as an extracellular vesicle), the VP4 spike protein must be cleaved by a protease, which results in the proteins VP5* and VP8* (Arias, Romero et al. 1996). Because they comprise the outer layer of the virion, VP7 and VP4 are capable of eliciting neutralizing antibodies, and are used to define G (glycoprotein) and P (protease sensitive) serotypes respectively (Matthijnssens, Ciarlet et al. 2008, Nair, Feng et al. 2017). Consequently, VP7 and VP4 are likely to be under strong selection for diversification to mediate cell entry or escape host immune responses (McDonald, Matthijnssens et al. 2009, Kirkwood 2010, Patton 2012).

Based on sequence identity and antigenic properties of VP6, 10 different rotavirus groups (A–J) have been identified, with group A rotaviruses being the most common cause of human infections (Matthijnssens, Otto et al. 2012, Mihalov-Kovacs, Gellert et al. 2015, Banyai, Kemenesi et al. 2017). A genome classification system based on established nucleotide percent cutoff values has been developed for group A rotaviruses (Matthijnssens, Ciarlet et al. 2008, Matthijnssens, Ciarlet et al. 2011). In the classification system, the segments VP7-VP4-VP6-VP1-VP2-VP3-NSP1-NSP2-NSP3-NSP4-NSP5/6 are represented by the indicators Gx-P[x]-Ix-Rx-Cx-Mx-Ax-Nx-Tx-Ex-Hx, (x = Arabic numbers starting from 1), respectively (Matthijnssens, Ciarlet et al. 2008, Matthijnssens, Ciarlet et al. 2011). To date, between 20 to 51 different genotypes have been identified for each segment, including 51 different VP4 genotypes (P[1]–P[51]) and 36 different VP7 genotypes (G1–G36), both at 80% nucleotide identity cutoff values (Steger, Boudreaux et al. 2019).

The propensity of rotavirus for coinfection and outcrossing with other rotavirus strains makes it a difficult pathogen to control and surveil, even with current vaccines (Rahman, Matthijnssens et al. 2007, Matthijnssens, Ciarlet et al. 2008, Matthijnssens, Bilcke et al. 2009, Kirkwood 2010, Ghosh and Kobayashi 2011, Sadiq, Bostan et al. 2018). Understanding rotaviral diversity expansion, genetic exchange between strains (especially between the clinically significant type I and type II genogroups), and evolutionary dynamics resulting from coinfections have important implications for disease control (Rahman, Matthijnssens et al. 2007, Matthijnssens, Ciarlet et al. 2008, Matthijnssens, Bilcke et al. 2009, Kirkwood 2010, Ghosh and Kobayashi 2011, Sadiq, Bostan et al. 2018). Rotavirus A genomes have high mutation rates (Matthijnssens, Heylen et al. 2010, Donker and Kirkwood 2012, Sadiq, Bostan et al. 2018), undergo frequent reassortment (Ramig and Ward 1991, Ramig 1997, Ghosh and Kobayashi 2011, McDonald, Nelson et al. 2016), and the perception is that these two processes are the primary drivers of rotavirus evolution (Doro, Farkas et al. 2015, Sadiq, Bostan et al.

2018). Genome rearrangements may also contribute to rotavirus diversity, but are not believed to be a major factor in rotavirus evolution (Desselberger 1996). Homologous recombination, however, is thought to be especially rare in rotaviruses due to their dsRNA genomes (Ramig 1997, McDonald, Nelson et al. 2016, Varsani, Lefeuvre et al. 2018). Unlike +ssRNA (Lukashev 2005) viruses and DNA viruses (Pérez-Losada, Arenas et al. 2015), dsRNA viruses cannot easily undergo intragenic recombination because their genomes are not replicated in the cytoplasm by host polymerases, but rather within nucleocapsids by viral RNA-dependent RNA polymerase (Ramig 1997, Patton, Vasquez-Del Carpio et al. 2007). Genome encapsidation should significantly reduce the opportunities for template switching, the presumptive main mechanism of intramolecular recombination (Lai 1992, Pérez-Losada, Arenas et al. 2015).

Despite the expectation that recombination should be rare in rotavirus A, there are nevertheless numerous reports of recombination among rotaviruses in the literature (Suzuki, Gojobori et al. 1998, Parra, Bok et al. 2004, Phan, Okitsu et al. 2007, Phan, Okitsu et al. 2007, Cao, Barro et al. 2008, Martinez-Laso, Roman et al. 2009, Donker, Boniface et al. 2011, Jere, Mlera et al. 2011, Esona, Roy et al. 2017, Jing, Zhang et al. 2018). However, a comprehensive survey of 797 rotavirus A genomes failed to find any instances of the same recombination event in multiple samples (Woods 2015). There are two possible explanations for this outcome. Either the putative recombinants were spurious results stemming from poor analytical technique or were poorly fit recombinants that failed to increase in frequency in the population such that they would be resampled (Woods 2015). The main implications of this study are that recombination among rotavirus A is rare, usually disadvantageous, and not a significant factor in rotavirus evolution.

Since the number of publicly available rotavirus A whole segment genomes is now over 23,600, it is worth revisiting these conclusions to see if they are still valid. To this end, we used bioinformatics tools to identify possible instances of recombination among all available complete rotavirus A genome sequences available in the NCBI Virus Variation database as of May, 2019. We found strong evidence for recombination events among all rotavirus A segments with the exception of NSP3 and NSP5. In several cases, the recombinants were fixed in the population such that several hundred sampled strains showed remnants of this same event. These reports suggest that rotavirus recombination occurs more frequently than is generally appreciated, and can significantly influence rotavirus A evolution.

Methods

Sequence Acquisition and Metadata Curation

We downloaded all complete rotavirus genomes from NCBI's Virus Variation Resource as of May 2019 (n = 23,627) (Hatcher, Zhdanov et al. 2017). Laboratory strains were removed from the dataset. Genomes that appeared to contain substantial insertions were excluded as well. Avian and mammalian strains were analyzed separately as recombination analyses between more divergent genomes can sometimes confound the results. No well-supported events were identified among the avian strains. For each rotavirus genome, separate fasta files were downloaded for each of the 11 segments. Metadata including host, country of isolation, collection date, and genotype (genotype cutoff values as defined by (Matthijnssens, Ciarlet et al. 2008)) were recorded. The

genotype cutoff values allowed for the differentiation of events that occurred between two different genotypes—intergenotypic—from those which occurred between the same genotype—intragenotypic.

Recombination Detection and Phylogenetic Analysis

All 11 segments of each complete genome were separately aligned using MUSCLE v3.8.31 (Edgar 2004) after removing any low quality sequence (e.g., 'Ns'). Putative recombinants were identified using RDP4 Beta 4.97, a program, which employs multiple recombination detection methods to minimize the possibility of false positives (Martin, Murrell et al. 2015). All genomes were analyzed, with a p-value cut off < 10E-4, using 3Seq, Chimæra, SiScan, MaxChi, Bootscan, Geneconv, and RDP as implemented in RDP4 (Martin, Murrell et al. 2015). We eliminated any strains that did not show a putative recombination event predicted by at least 6 of the above listed programs. We then ran separate phylogenic analyses on the 'major parent' and 'minor parent' sequences of putative recombinants in BEAST v1.10.4 using the general time reversible (GTR) + Γ + I substitution model (Suchard, Lemey et al. 2018). 'Parent' in this case does not refer to the actual progenitors of the recombinant strain, but rather those members of the populations whose genome sequences most closely resemble that of the recombinant. Significant phylogenetic incongruities with high posterior probabilities between the 'major parent' and 'minor parent' sequences were interpreted as convincing evidence for recombination.

Phylogenetic Analysis of VP1 and VP3

Segment 1 (VP1) and segment 3 (VP3) each showed evidence for recombination events resulting in a novel lineage, wherein many isolates reflected the same recombination event. To analyze these events more thoroughly, we split alignments of a subset of environmental isolates to include flagged clades, minor parent clades, and major parent clades along with outgroup clades to improve accuracy of tip dating. We generated minor and major parent phylogenies using BEAST v1.10.4 (Suchard, Lemey et al. 2018). We used tip dating to calibrate molecular clocks and generate time-scaled phylogenies. The analyses were run under an uncorrelated relaxed clock model using a time-aware Gaussian Markov random field Bayesian skyride tree prior (Minin, Bloomquist et al. 2008). The alignments were run using a GTR + Γ + I substitution model and partitioned by codon position. Log files in Tracer v1.7.1 (Rambaut, Drummond et al. 2018) were analyzed to confirm sufficient effective sample size (ESS) values, and trees were annotated using a 20% burn in. The alignments were run for three chains with a 200,000,000 Markov chain Monte Carlo (MCMC) chain length, analyzed on Tracer v1.7.1 (Rambaut, Drummond et al. 2018), and combined using LogCombiner v1.10.4 (Drummond and Rambaut 2007). Trees were annotated with a 10% burn, and run in TreeAnnotator v1.10.4 (Suchard, Lemey et al. 2018). The best tree was visualized using FigTree v1.4.4 (Rambaut 2019) with the nodes labeled with posterior probabilities.

RNA Secondary Structure Analysis

To test the hypothesis that recombination junctions were associated with RNA secondary structure, we generated consensus secondary RNA structures of different segments and genotypes using RNAalifold in the

ViennaRNA package, version 2.4.11 (Bernhart, Hofacker et al. 2008, Lorenz, Bernhart et al. 2011). The consensus structures were visualized and mountain plots were generated to identify conserved structures that may correspond to breakpoint locations. We made separate consensus alignments in two ways, by using the same genotype and by combining genotypes. Due to the high sequence variability of the observed recombinants, particularly in segments 4 (VP4) and 9 (VP7), we note that the consensus structures may vary substantially depending on the sequences used in the alignments. Segments 7 (NSP3), 10 (NSP4), and 11 (NSP5) were not analyzed due to only having one or no recombination events. Consensus structures could not reliably be made for segment 2 (VP2). While the VP2 protein is relatively conserved across genotypes, it contains insertions particularly in the C1 genotype, yet shows recombination across C1 and C2 genotypes.

Protein Structure and Antigenic Epitope Predictions

To evaluate whether recombination events resulted in substantial (deleterious) protein structure changes, we employed LOMETS2 (Local Meta-Threading-Server) I-TASSER (Iterative Threading Assembly Refinement) (Zhang 2008, Roy, Kucukural et al. 2010, Yang and Zhang 2015) to predict secondary and tertiary protein structures. I-TASSER generates a confidence (C) score for estimating the quality of the protein models. To determine if any of the putative recombinants possessed recombined regions containing epitopes, we analyzed the amino acid sequences of all VP4, VP6, and VP7 recombinants and their major and minor parents. We used the Immune Epitope Database (IEDB) (Vita, Mahajan et al. 2019) and SVMTriP (Yao, Zhang et al. 2012) to predict conserved epitopes.

Results

Strong Evidence for Homologous Recombination in Rotavirus A

We identified 109 putative recombination events (identified by 6/7 RDP4 programs; Table 1, Supplementary Table 1). Of these, 67 recombination events were strongly supported, meaning they were detected by 7/7 RDP4 programs with a p-value cut off < 10E-9 (Table 1). Most recombination events detected were observed in sequences uploaded to the Virus Variation database since the last large scale analysis (Woods 2015) so differences between these results and prior studies may simply reflect the recent increase in available genome sequences.

Putative Recombination Events Observed in Multiple Environmental Isolates

Eleven of the recombination events identified in Table 1 were observed in more than one environmental isolate (Fig. 1; Table 2). The observation of multiple sequenced strains with the same recombination event is strong evidence that the observed event was not spurious, and was not a consequence of improper analytical technique or experimental error. Assuming the events are not spurious, there are only two ways that multiple sequenced isolates will show the same recombinant genotype. Either multiple recombination events with the same exact breakpoints occurred at approximately the same time, or the event happened once and descendants of the recombined genotype were subsequently isolated from additional infected hosts. The latter scenario is more parsimonious, and suggests that the new genotype was not reproductively impaired. Indeed, some

recombined genotypes may be more fit than their predecessors, but this outcome would need to be experimentally validated with infectivity assays.

Table 1. *Recombination events identified among all mammalian rotavirus A genome sequences downloaded from NCBI Virus Variation database in May 2019 (Hatcher, Zhdanov et al. 2017).* [a]*6/7 programs implemented in RDP4 identified putative recombination event (see Methods).* [b]*Events identified by 7/7 programs implemented in RDP4 or events where more than one environmental isolate showed the same event (see Methods).* [c]*Strongly supported events (Row 3) divided by number of sequences analyzed (Row 1).* [d]*Number of intergenotypic events out of all putative recombination events (Row 2).*

	VP1	VP2	VP3	VP4	VP6	VP7	NSP1	NSP2	NSP3	NSP4	NSP5
Number of sequences analyzed	1710	1600	1905	1990	2176	3887	1962	2186	1881	2430	1900
Putative recombination events[a]	15	13	16	11	11	24	11	4	0	3	1
Strongly supported events[b]	7	8	15	7	6	14	7	1	0	1	1
Recombination frequency[c]	4.1E-3	5.0E-3	7.9E-3	3.5E-3	2.8E-3	3.6E-3	3.6E-3	4.6E-4	--	4.1E-4	5.3E-4
Intergenotypic recombination ratio[d]	2/15	8/13	4/16	6/11	7/11	22/24	3/11	2/4	--	2/3	1/1

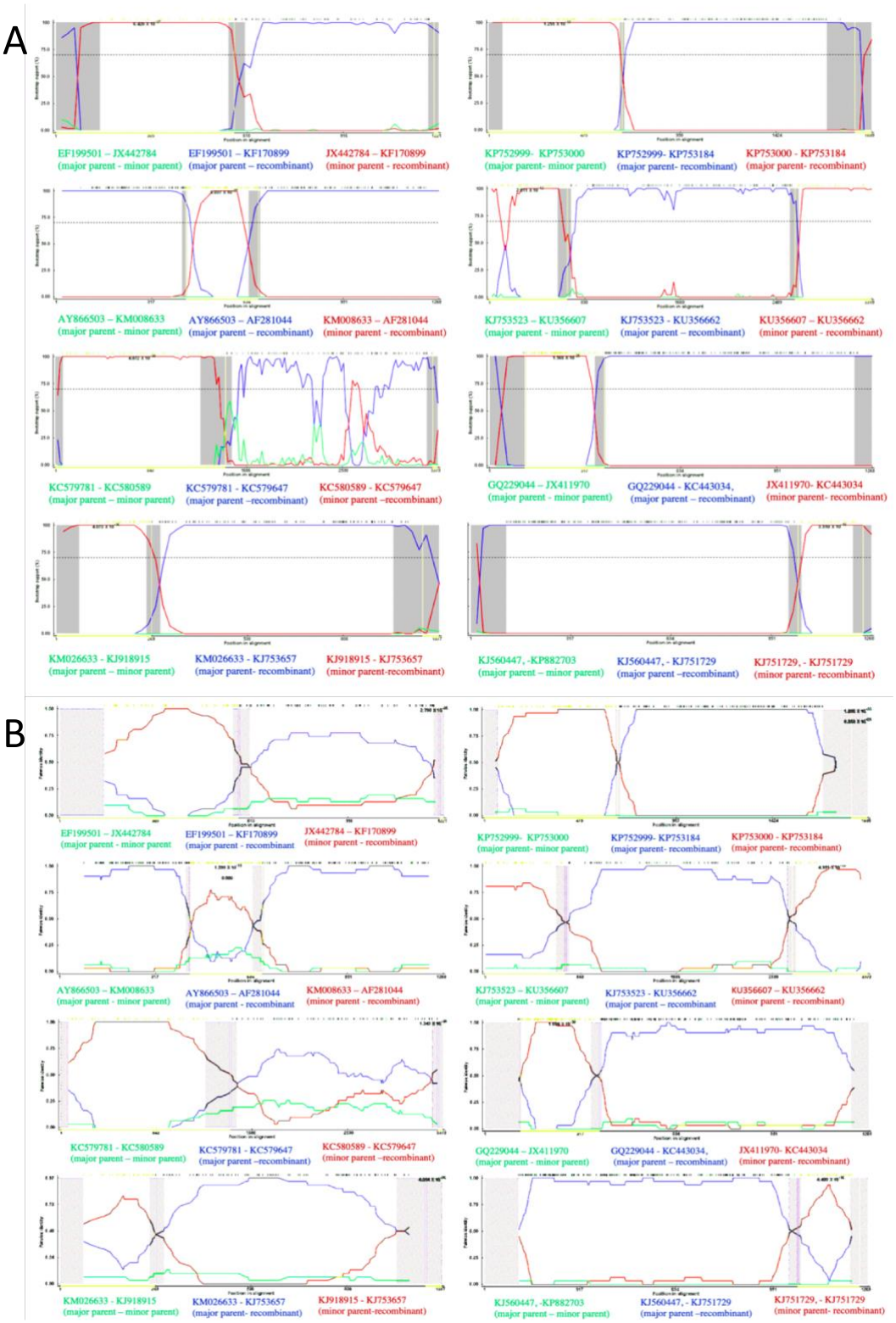

Figure 1. *Bootscan (A) and RDP (B) analyses of putative recombinants where multiple environmental samples supported the event. From top left to bottom left: a G6-G6 event in VP7, a G9-G1 event, an R1-R1 event in VP1, and an N1-N1 event in NSP2. From top right to bottom right: an A8-A8 event in NSP1, an R2-R2 event in VP1, a G2-G1 event in VP7, and a G3-G1 event.*

***Table 2**. Recombination events observed in multiple independent environmental isolates (i.e., isolates from different patients and/or sequenced by different laboratories). [a]99% confidence intervals. [b]See Fig. 2.*

Recombined Segment	Genotype(s) Involved	Number of Independent Isolates	Corrected and Uncorrected Multiple Comparisons	Breakpoints[a]	Accession Numbers
Segment 1 (VP1)	R1	2	4.787E-18 and 1.349E-10	35 – 1448 (1290 –1498)	KC579647 KC580176
Segment 1 (VP1)	R2	Flagged in 285 samples.	1.305E-16 and 3.332E-09	(541-711) – (1327–1445)	KU199270[b]
Segment 1 (VP1)	R2	2	1.756E-20 and 4.951E-13	656 (541–711) – 2661 (2600–2735)	KU356662 KU356640
Segment 3 (VP3)	M2	Flagged in 551 samples.	1.78E-12 and 4.982E-05	1258 (872–1389) – 1798 (1662–1917)	KX655453
Segment 3 (VP3)	M1	Flagged in 107 samples.	2.491E-20 and 6.946E-13	2158 (2129–2174) – 2531 (undetermined)	KJ919553 KJ919517 KJ919551 KJ753665 JQ069727
Segment 7 (NSP1)	A8 (porcine)	3	3.01E-37 and 8.622E-30	(1434–25) – (573–596)	KP753174 KJ753184 KP752951
Segment 8 (NSP2)	N1	3	3.689E-13 and 4.054E-06	485 (455–499) – 889 (868–914)	KJ753657 KM026663 KM026664
Segment 9 (VP7)	G6 (bovine)	2	6.240E-12 and 2.780E-05	1048 (1032–128) – 481 (448–506)	HM591496 KF170899
Segment 9 (VP7)	G1 & G2	2	5.507E-38 and 1.664E-30	55 (994–60) – 291 (262–296)	KC443034 MG181727
Segment 9 (VP7)	G1 & G3	2	1.4E-23 and 4.230E-16	857 (833–859) – 1019 (991–51)	KJ751729 KP752817
Segment 9 (VP7)	G1 & G9	2	5.292E-19 and 1.599E-11	362 (346–366) – 589 (558–605)	AF281044 GQ433992

Segment 1 Intragenotypic Recombination Resulting in a New Lineage

Segment 1 (VP1; ~3,302 base pairs) showed evidence of a recombination event within the R2 clade that was fixed in the population, and resulted in a new lineage (highlighted clade in Fig. 2; Fig. 3; Table 2). The multiple comparison (MC) uncorrected and corrected probabilities were 1.305E-16 and 3.332E-09 respectively. The sequence most closely related to the recombined sequence was KU199270, a human isolate from Bangladesh in 2010 (Aida, Nahar et al. 2016). Phylogenetic analysis using tip calibration suggests that the recombination event occurred no later than 2000-2005 (node Cis), so if this is a true recombination event, the 2010 sequence is not the original recombinant. The recombinant region is 100% similar to an isolate also from Bangladesh in 2010 (KU248372) (Aida, Nahar et al. 2016), which also has a putative recombinant sequence in another region of its genome. The breakpoint regions (99% CI: (541-711) — (1327-1445)) may represent a potential hotspot for segment 1 recombination as multiple recombination events show breakpoints in this area

(Table 2). Phylogenetic analysis of the alignment of 250 representative sequences containing only the putative recombinant region compared with the rest of the segment 1 sequence showed a consistent subclade shift within the R2 clade. The recombination events resulted in the incorporation of the following amino acid substitutions in the recombinant strains when compared to the major parent strain: 227 (K→E), 293 (D→N), 297 (K→R), 305 (N→K), and 350 (K→E).

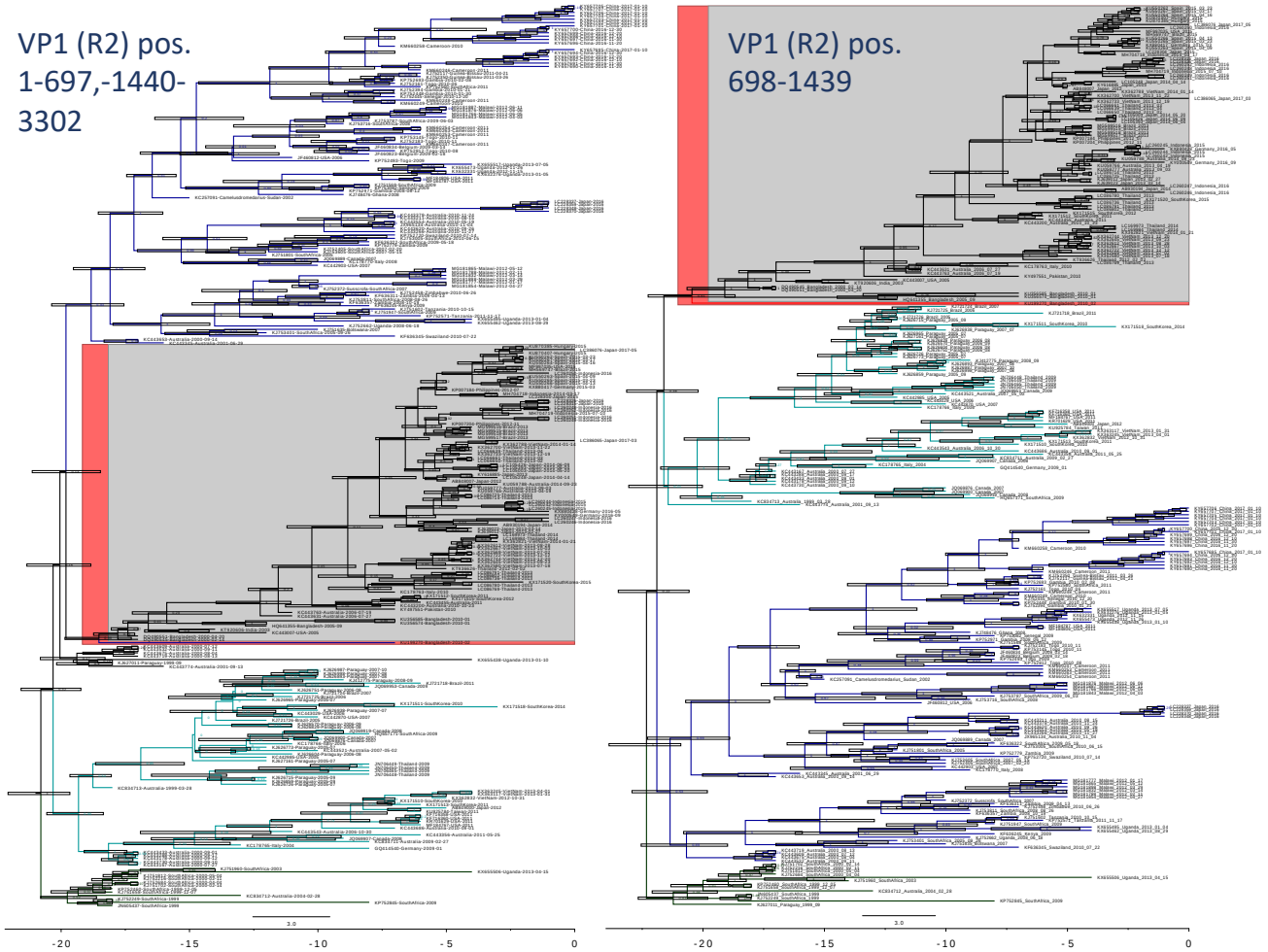

Figure 2. *Bayesian phylogenetic analysis of a possible recombination event in VP1 that became fixed in the population. The strain closest to the recombination event is highlighted in red. Major clades are colored to show the phylogenetic incongruity. Nodes are labeled with posterior probabilities with 95% node height intervals shown. Time axis at the bottom is in years before 2017.*

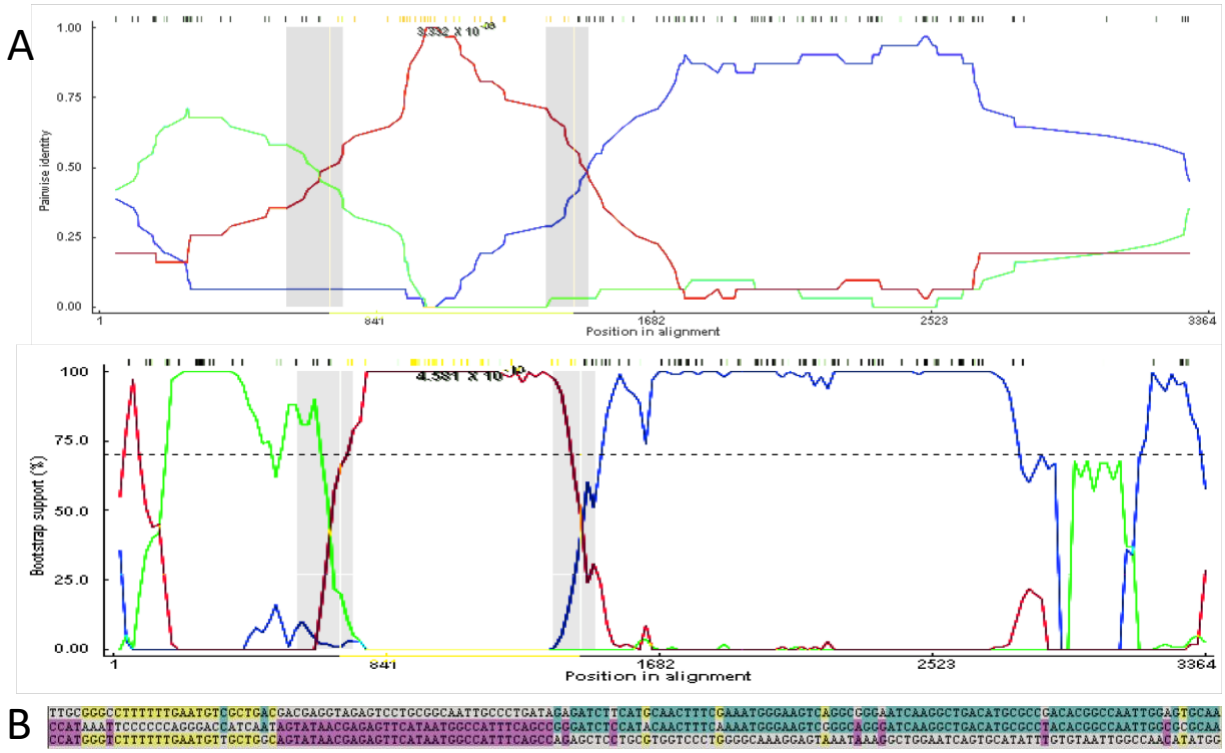

Figure 3*. A) An RDP analysis (top) and a BootScan analysis (bottom) showing a putative recombination event between two R2 segment 1 genotypes. The red line compares the minor parent to the recombinant, blue line compares the major parent to the recombinant, and the green line compares the major parent to the minor parent. The Y-axis for RDP (top) is the pairwise identity, while the Y-axis for BootScan (bottom) is the bootstrap support. The X-axis is the sequence along segment 1. B) The relevant sites shown above color-coded to strain that the recombinant matches. The recombinant is the middle sequence, the minor parent is the bottom sequence, and the major parent is the top sequence. Mutations matching the major sequence are shown in blue, while mutations matching the minor parent are shown in purple. Yellow mutations show mutations not present in the recombinant sequence but which match the major and minor parent, possibly suggesting a second recombination event.*

Segment 3 Intragenic Recombination

Two recombination events occurring in segment 3 (VP3) appear to have fixed in the population, and are seen in many descendant sequences (Table 2). The first strain identified as a putative recombinant is KJ753665, an isolate from South Africa in 2004. The recombinant region occurs between positions (2129-2174) — 2531. This region is 98.7% identical to a porcine strain isolated in Uganda in 2016 (KY055418)(Bwogi, Jere et al. 2017), while the rest of segment 3 is 95.8% similar to a 2009 human isolate from Ethiopia (KJ752028). The Monte Carlo uncorrected and corrected probabilities were 2.491E-20 and 6.946E-13, respectively, with 107 isolates flagged as possibly derived from the recombination event. Phylogenetic analysis using 450 randomly selected VP3 sequences (excluding sequences lacking collection dates) within the putative recombinant region, along with an analysis of the genome excluding the two major recombination events, resulted in five sequences showing a significant phylogenetic incongruity (Fig. 4). The incongruity appeared between sub-lineages within

the larger M1 lineage of VP3. Amino acid substitutions in the recombinant region included positions 748 (M→T) and 780 (T→M).

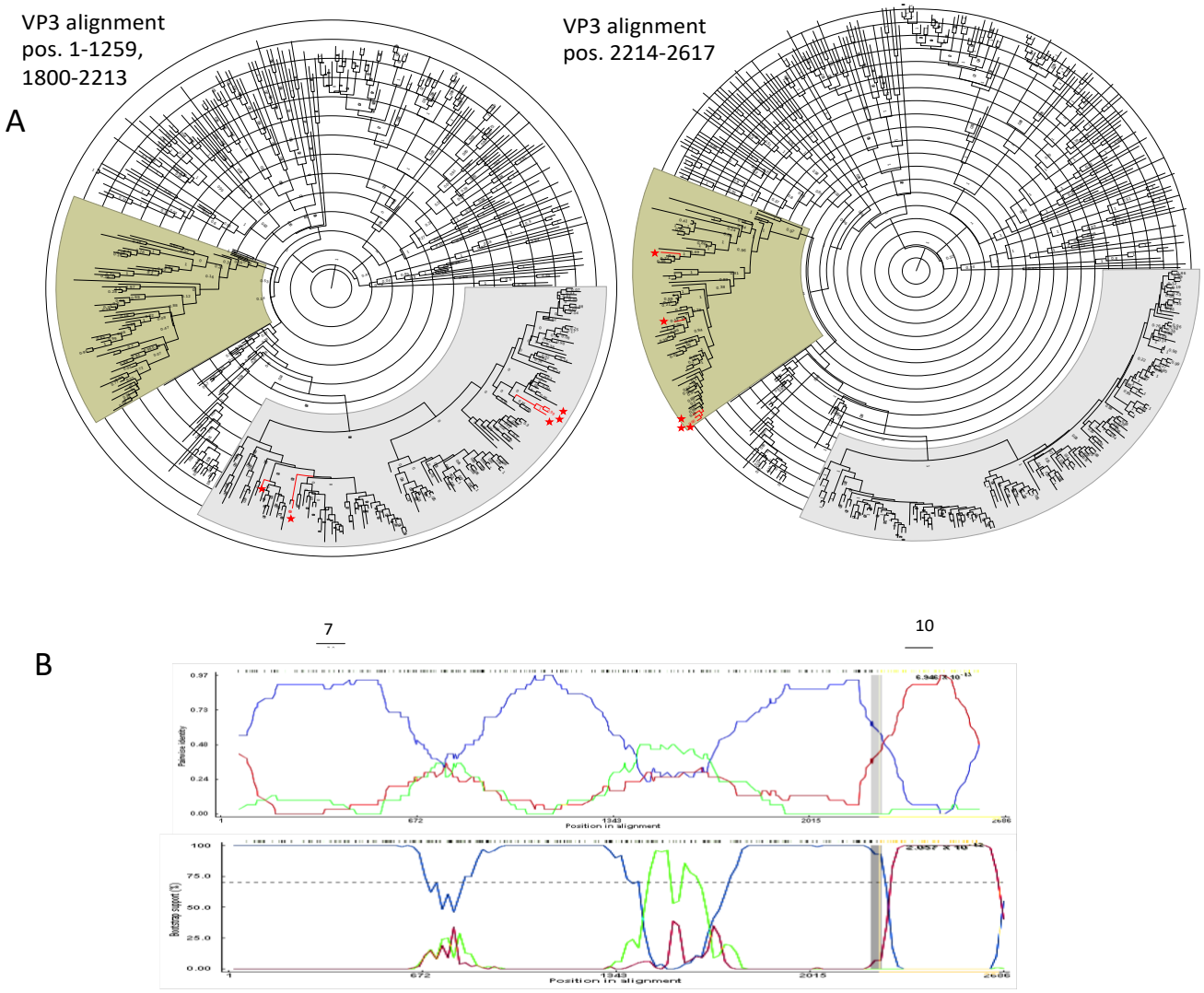

Figure 1. *Segment 3 recombination event supported by multiple isolates. A) Phylogenetic trees made using alignments from (left) nucleotide positions 1-1259 and 1800-2213 representing the major parent region excluding second recombination event (Fig. 5), and (right) nucleotide position 2214-2617 representing the minor parent sequence. B) BootScan (top) and RDP (bottom) analyses. The red line compares the minor parent to the recombinant, blue line compares the major parent to the recombinant, and the green line compares the major parent to the minor parent. The Y-axis for the BootScan analysis (top) is the bootstrap support, while the Y-axis for the RDP analysis (bottom) is the pairwise identity. The X-axis for both analyses is the sequence along segment 3.*

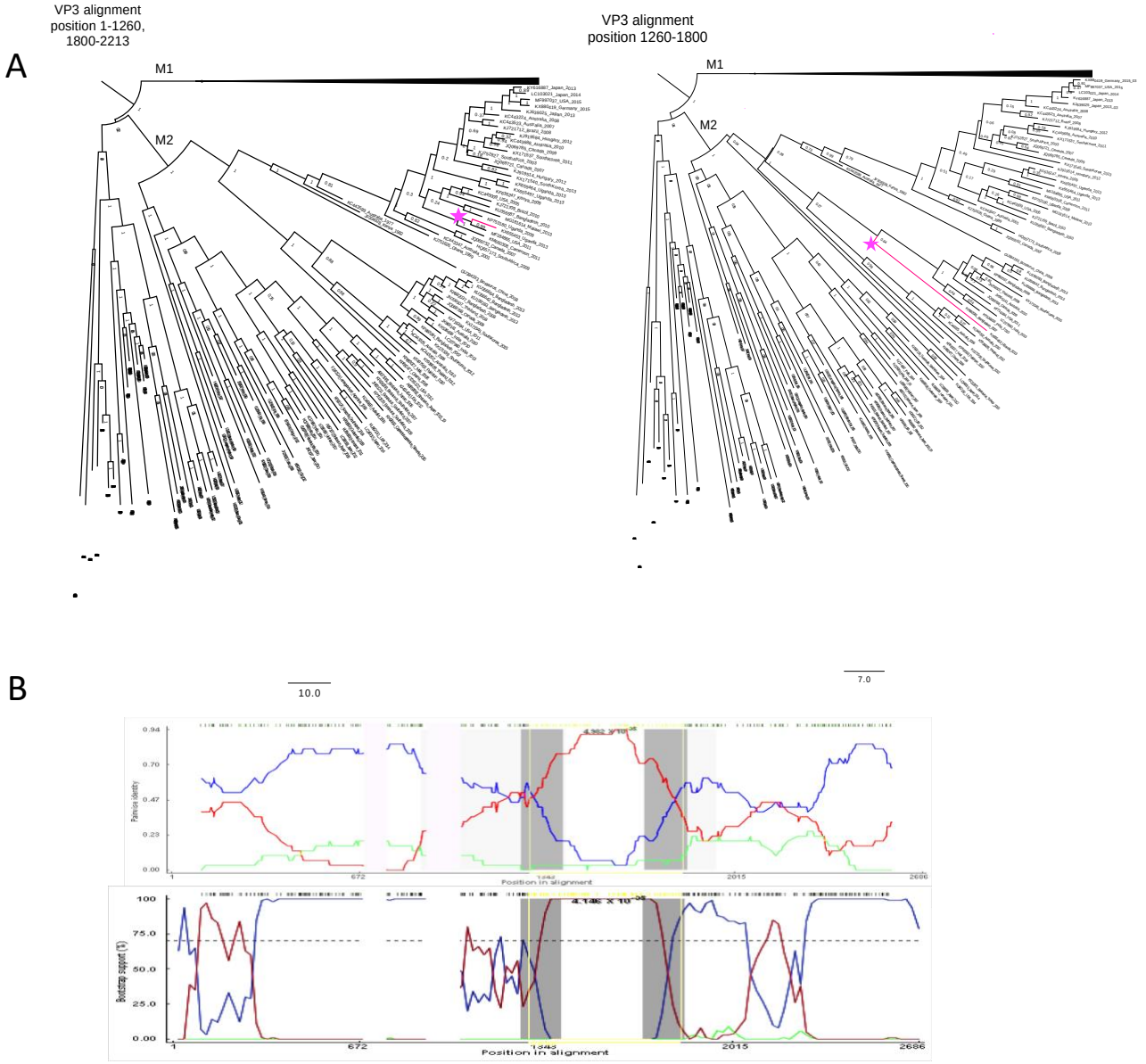

Figure 5. *A) Phylogenetic analysis of segment 3. Left tree (major parent) was made from an alignment of nucleotide positions 1-1260 and 1900-2213 and right tree (minor parent) was made from nucleotide positions 1260-1800. M2 strains have been collapsed, and recombinant is colored in pink. B) BootScan (top) and RDP analyses (bottom of VP3 M2 putative recombinant. The red line compares the minor parent to the recombinant, blue line compares the major parent to the recombinant, and the green line compares the major parent to the minor parent. The Y-axis for BootScan is the bootstrap support, while the Y-axis for the RDP analysis is the pairwise identity. The X-axis in both analyses is the segment 3 sequence.*

A second potential recombination event was identified in segment 3 between sublineages within the M2 lineage (Table 2; Fig. 5). However, when we created split alignments and ran a phylogenetic analysis in BEAST v1.10.4, only one sequence showed a phylogenetic incongruity supporting this event (KX655453). Amino acid substitutions as a result of this event included positions 405 (I→V), 412 (V→M), 414 (N→D), 441 (N→D), 458 (I→V), 459 (I→T), 468 (L→F), 473 (N→D), 486 (M→I), 518 (N→S), and 519 (E→G).

One possible complication with relying on phylogenetic incongruity as evidence of major recombination events is that a recombinant virus may evolve faster than the parental strains, and, despite possessing an initial fitness advantage such as immune avoidance, may eventually converge back towards the major parent's sequence. Thus, phylogenetic analysis likely underestimates the frequency of transiently stable recombination events in a population. This phenomenon may account for the observation that the number of VP3 isolates flagged as deriving from a recombination event based on sequence analysis is greater than the prevalence of recombination predicted by the phylogenetic analysis.

Intergenotypic Recombination

We found strong evidence for intergenotype recombination in all segments except segment 7 (NSP3) and segment 11 (NSP5) (Table 1; Supplementary Table 1). Instances of intergenotypic recombination in segment 1 (VP1) (KU714444, JQ988899) only occurred in regions where the amino acid sequence was highly conserved across genotypes, so these events resulted in few, if any, nonsynonymous mutations**.** Of the putative events observed in more than two environmental isolates with strong support from detection methods, only events in segment 9 (VP7) occurred between different genotypes (Table 2). The segment 9 recombinant region amino acid substitutions that match the minor parent and differ from the major parent are shown in Supplementary Table 2.

Structural Prediction of Recombinant Proteins

The protein models generated by I-TASSER for the intergenotypic recombinant G proteins showed that, although the amino acid changes for the G1-G2 recombinant were substantial (25 changes) (Supplementary Table 2), the secondary and tertiary structures seemed largely intact (Fig. 6). The G3-G1 and G6-G6 recombinants each showed four amino acid changes. The G9-G1 recombinant showed the most secondary structure disruption, including a loss of beta sheets, a loss of antiparallel beta sheets, and slightly shorter beta sheets/helices, which could indicate lower stability. However, based on the structural modeling, the tertiary structure appeared to be maintained, suggesting that the putative recombinant glycoproteins were able to form properly folded G-proteins (Fig. 6).

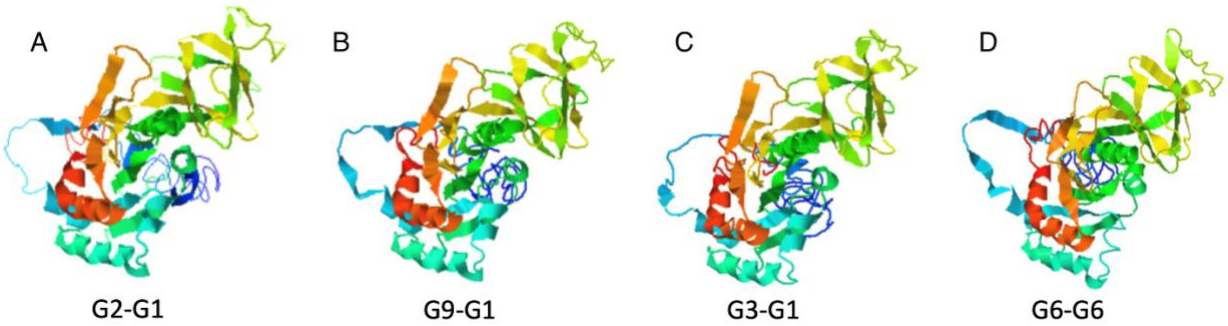

Figure 6. *VP7 protein structures were predicted from amino acid alignments of the four strongly supported G recombinants using I-TASSER. C-scores are confidence scores estimating the quality of the predicted model, and range from [-5, 2], with higher scores indicate greater confidence A) G2-G1,*

C-score = -1.38, KC443034; B) G9-G1:AF281044, C-score = -1.29; C) G3-G1, C-score = -1.27 KJ751729; D) G6-G6: KF170899, C-score = -1.42.

Antigenic epitope predictions generated by IEDB (Vita, Mahajan et al. 2019) and SVMTriP (Yao, Zhang et al. 2012), as well as a large study done on mammalian G-types (Ghosh, Chattopadhyay et al. 2012), showed that VP7 recombination occasionally results in amino acid substitutions in conserved epitopes (Supplementary Table 2). For example, the amino acid sequence RVNWKKWWQV is usually flagged as, or part of, an epitope in most G types including G2, G3, G4, G6, G9, but not in G1. In the G2-G1 recombination event flagged in multiple isolates (Table 2; Figure 1), this region is altered (sometimes a KR substitution and sometimes multiple amino acid substitutions) (Supplementary Table 2). Moreover, despite containing highly variable regions, the region where the recombination occurred had low solvent accessibility. The G3-G1 recombinant had amino acid substitutions in two of four conserved epitope regions due to the recombination event. There was also a conserved epitope sequence around amino acids 297-316 in G9 proteins that was altered in the G9-G1 recombinant so it no longer appeared as an epitope.

Structural predictions generated by I-TASSER suggest that, although the amino acid sequences may diverge, the protein folding and three-dimensional structures remain relatively conserved (Fig. 6). Thus, although the amino acid sequence substitutions do not result in significant changes to the protein structure, they may nevertheless reduce binding by antibodies or T-cell receptors, and may provide a selective advantage in allowing the virus to avoid immune surveillance.

Recombination Junctions Often Correspond to RNA Secondary Structure Elements

Breakpoint distribution plots showed the sequence regions with the most breakpoints. These breakpoints often corresponded to hairpins predicted by RNAalifold. Secondary RNA structure predictions for segment 9 (VP7) genotypes G1, G2, G6 and G9 are shown as mountain plots (Fig. 7). The breakpoints of the segment 9 recombination events correspond to areas leading to the peaks in the mountain plots (Fig. 7). The peaks indicate a conserved hairpin loop, with the sequences leading up to the peak being the double-stranded portion of the hairpin. Breakpoint distributions also appeared to correspond to secondary structure predictions made from alignments of segment 1 (VP1) and segment (VP6) (Fig. 8). Segment 4 (VP4) RNA secondary structure predictions (Supplementary Fig. 1) showed greater variation across genotypes, so while breakpoints did coincide with secondary RNA structures as predicted by the models, there were not enough events in each genotype to provide strong support that the breakpoints were correlated with secondary structure. The breakpoint distributions for NSP1 and VP3 were also non-randomly distributed across the sequence (Supplementary Fig. 1), however secondary structure predictions from these alignments were not consistent, so are not shown (Supplementary Fig. 2).

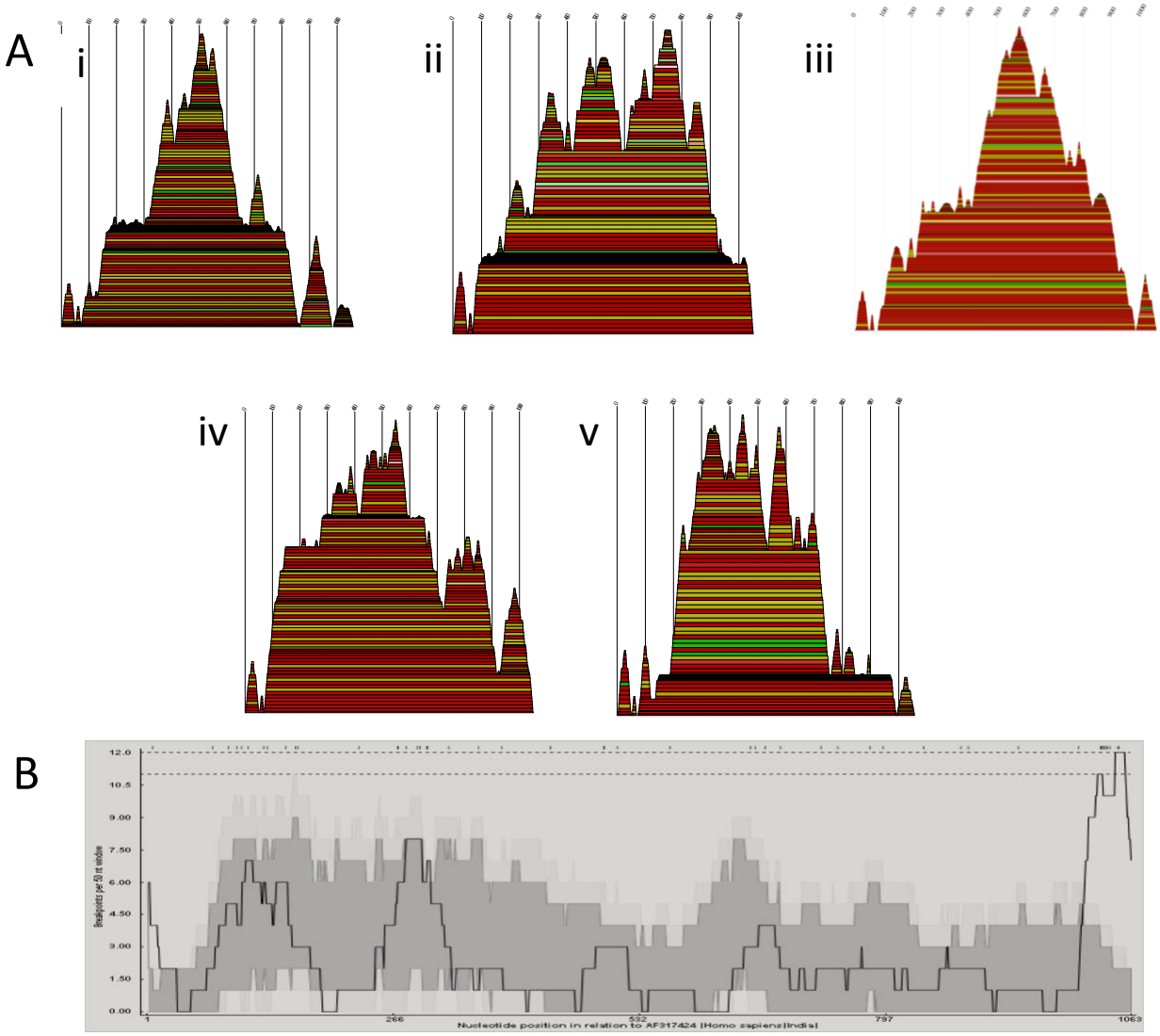

Figure 7. *A) Consensus mountain plots made in RNAalifold using the ViennaRNA package of the predicted RNA secondary structures based on alignments made using full sequences for each of the five segment 9 G types involved in the intergenotypic recombination events: (i) G9 (ii) G6 (iii) G3 (iv) G1 (v) G2. Peaks represent hairpin loops, slopes correspond to helices, and plateaus correspond to loops. The X-axis corresponds to the sequence of the segment. Each base-pairing is represented by a horizontal box where the height of the box corresponds with the thermodynamic likelihood of the pairing. The colors correspond to the variation of base pairings at that position. Red indicates the base pairs are highly conserved across all the sequences, and black indicates the least conservation of those base pairings. B) Breakpoint distribution plots made in RDP4 of putative recombinants in segment 9. The X-axis shows the position in the sequence, and Y-axis shows the number of breakpoints per 50 nucleotide window. The highest peaks are around X = 115, 285, 1050.*

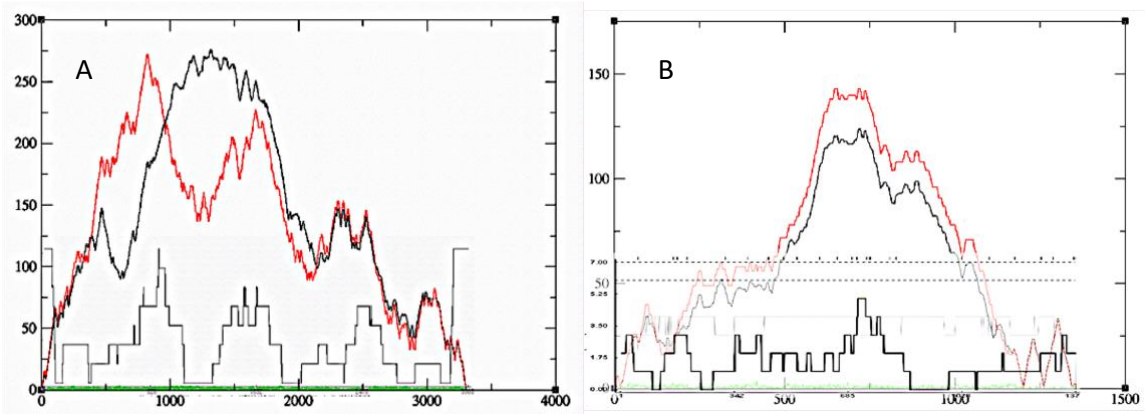

Figure 8. *Consensus mountain plots overlaid with breakpoint distribution plots for recombination events in A) VP6 and B) VP1. Position in the nucleotide sequence is on the X-axis. The entropy curve represented in green. The black curve represents the pairing probabilities, and the red curve represents the minimum free energy structure with well-defined regions having low entropy.*

Discussion

Detecting Recombination: Recognizing Type I and Type II Error

Apparent instances of recombination may actually be the result of convergent evolution, lineage-specific rate variation, sequencing error, poor sequence alignment, laboratory contamination or improper bioinformatics analysis (Worobey, Rambaut et al. 2002, Boni, de Jong et al. 2010, Bertrand, Töpel et al. 2012, Boni, Smith et al. 2012). Several steps can be taken to minimize incorrect attribution of viral recombination. Ideally this process should begin at the time of sequencing. First, it should be confirmed that the originating sample did not come from a host infected with multiple genotypes of the same virus type. Prior to RNA extraction, single plaques should be repeatedly picked and plated (i.e. plaque purification) to ensure that multiple genotypes are not inadvertently sequenced. Similarly, care must be taken when sequencing multiple samples of the same virus to minimize the possibility of cross-contamination.

For sequences obtained from online repositories, such precautions are rarely possible. Instead careful bioinformatics procedures can help minimize possible errors. As typical first step in identifying recombination events, virus genome sequences are analyzed with software such as RDP4 (Martin, Murrell et al. 2015), but all software programs are prone to error. For example, programs may falsely identify a recombination event when none exists (type I error) or fail to detect a true recombination event when one exists (type II error). Several studies measured errors incurred by RDP4 in the analysis of the genomes of tick-borne encephalitis virus, a positive-sense RNA flavivirus that rarely recombines (Norberg, Roth et al. 2013, Bertrand, Johansson et al. 2016). The results of the analyses indicated that recombination was overestimated in these viruses, and that certain detection methods were more prone to type I error (Norberg, Roth et al. 2013, Bertrand, Johansson et al. 2016). MaxChi, Chimaera, and SiScan showed higher false positive rates than other RDP4 programs, but had greater power to detect true recombination events. By contrast, 3Seq and GENECONV displayed lower false positive rates, but had the lowest detection power of true events.

False positives using RDP4 are especially common among closely related strains (Bertrand, Johansson et al. 2016). That said, recombination events are likely occur between closely related strains given their close spatial/temporal proximity and genetic compatibility, so caution should be used in inferring events between highly dissimilar genotypes. When a positive recombination signal has been detected, it is essential to assess its statistical significance. However, in RDP4, the *P*-value of 0.05 does not correspond to a 5% rate of false positives (Bertrand, Johansson et al. 2016), therefore we used a cut-off value of 10E-04 and focused only on events where at least six RDP4 programs detected the putative recombinant.

After identifying putative recombination events, additional strategies can be used to eliminate errors. For example, rates of type I and type II error increase with shorter length recombination regions (Boni, Zhou et al. 2008, Norberg, Roth et al. 2013, Bertrand, Johansson et al. 2016). Therefore, we ignored any putative recombination events of < 100nt with the exception of one isolate in segment 4 (NSP4) and one isolate in segment 5 (NSP5) as the putative recombinant regions in these isolates were in conserved regions at the ends of the respective segments (Supplementary Table 1). In addition, we visually inspected sequence alignments to exclude misaligned sequences (Boni, de Jong et al. 2010). Splitting alignments by major and minor parent followed by carefully parameterized BEAST runs may help distinguish genuine phylogenetic incongruity signals from spurious false positives. Furthermore, we checked for the presence of unique polymorphisms differing from the parent strains within the suspected recombination region as they may provide evidence that recombination events are not laboratory artifacts. Presumably such substitutions would reflect subsequent adaptive evolution by the recombinant virus.

In addition, we noted how many times the same recombination event occurred across multiple samples since false positive recombinants are likely to be present as single isolates in phylogenetic trees (Boni, de Jong et al. 2010). The more isolates showing the same event, the greater the probability that it represents a true recombination event, especially if the isolates were acquired and sequenced by different laboratories. Events that showed strong support, but were only isolated in one sequence are noted (Supplementary Table 1), but not discussed, as it is difficult to rule out the possibility of type I error due to PCR or mosaic contig assembly (Boni, de Jong et al. 2010, Varsani, Lefeuvre et al. 2018).

Sequence metadata can also be used to identify unlikely recombination events. For an event to be plausible, the major and minor parents should have had opportunity to coinfect the same host, which is only possible if they are congruent in time and space (Boni, de Jong et al. 2010). For example, one study identified influenza A virus strain A/Taiwan/4845/99 as a recombinant of A/Wellington/24/2000 and A/WSN/33 (He, Han et al. 2008). Given that the two parents were isolated 77 years apart in different parts of the world, it is exceedingly unlikely that is a natural recombination event. Any putative recombination events should be carefully screened to determine if the parental strains could have plausibly interacted. In Supplementary Table 1, we include information on source species, year and place of isolation, % average nucleotide identity, and genogroup for all putative recombinants and their major and minor parents.

Naturally High Coinfection in Rotavirus A

Some features of rotavirus biology make recombination not only possible, but also relatively plausible. Rotaviruses are often released from cells as aggregates of approximately 5-15 particles contained within extracellular vesicles (Santiana, Ghosh et al. 2018). While it is not yet clear whether these extracellular vesicles can contain different rotavirus genotypes, they do allow for rotavirus coinfection even at low multiplicities of infection. Thus, the physical barriers to recombination in dsRNA viruses (Lai 1992) may be offset by the high rates of coinfection resulting from vesicle transmission of rotaviruses.

Furthermore, infection of hosts by multiple rotavirus strains appears to be relatively common. In a study of 100 children in the Detroit area, G and P typing, which identifies the serotype of the VP7 and VP4 proteins respectively, revealed that ~10% of patients were infected with multiple rotavirus A strains (Abdel-Haq, Thomas et al. 2003). Similarly high frequencies of G and P mixed genotype infections were observed in children sampled in India (three studies showing multiple G types in 11.3 %, 12% and 21% of samples) (Husain, Seth et al. 1996, Jain, Das et al. 2001, Khetawat, Dutta et al. 2002), Spain (>11.4% of samples) (Sánchez-Fauquier, Montero et al. 2006), Kenya (5.9%) (Kiulia, Peenze et al. 2006), Africa (12%) (Mwenda, Ntoto et al. 2010), and Mexico (5.6% in 2010, 33.5% in 2012) (Anaya-Molina, De La Cruz Hernández et al. 2018). Even higher frequencies of mixed genotype infections were observed in whole genome studies. For example, among 39 Peruvian fecal samples genotyped using multiplexed PCR, 33 (84.6%) showed evidence of multiple rotavirus genotypes (Rojas, Dias et al. 2019). In another study, whole genome deep sequencing revealed that 15/61 (25%) samples obtained in Kenya contained multiple rotavirus genotypes (Mwanga, Nyaigoti et al. 2018). Given the high genetic diversity of rotavirus populations (Kirkwood 2010, Ghosh and Kobayashi 2011, Sadiq, Bostan et al. 2018), and their proficiency in infecting a broad range of mammalian hosts including many domesticated animal species (Martella, Banyai et al. 2010, Doro, Farkas et al. 2015), the high frequencies of hosts infected with multiple genotypes is not entirely surprising. These coinfections present abundant opportunities for rotavirus recombination.

Rotavirus Recombination Generates Genetic Diversity

Homologous recombination previously has not been considered a significant driver in rotavirus genetic diversity and evolution (Ramig 1997, Woods 2015). Recombination is usually expected to be deleterious as the breakage of open reading frames may disrupt RNA secondary structure and alter protein functionality (Lai 1992, Simon-Loriere and Holmes 2011). However, recombination, as with reassortment (Ramig and Ward 1991, Iturriza-Gomara, Isherwood et al. 2001, Schumann, Hotzel et al. 2009, Ghosh and Kobayashi 2011, Jere, Chaguza et al. 2018), may further increase rotavirus genetic diversity due to epistatic interactions resulting in reassortant-specific or recombinant-specific mutations (Zeldovich, Liu et al. 2015). Formerly deleterious mutations may become beneficial when the genetic background changes, resulting in an increase in circulating pathogenically relevant viral strains.

In our study, most recombination events occurred between strains of the same genotype (Fig. 1; Table 2; Supplementary Table 1). This outcome is consistent with the expectation that intragenotypic is more common since it would less likely to disrupt protein or secondary RNA structure. Nonetheless, intragenotypic

recombination can have long lasting effects on rotavirus genetic diversity. For example, we identified a recombinant sub-lineage within the R2 clade of segment 1, the polymerase-encoding segment (Fig. 2; Fig. 3; Table 2). As the same event is found in strains isolated years apart from geographically distant locations, we can infer that the resulting genotype was sufficiently fit enough to be maintained in the population and disperse widely (Supplementary Table 1). This finding suggests that this homologous recombination event has had a long-term effect on rotavirus diversity.

While comparatively less common, we observed instances of intergenotypic recombination in all segments with the exception of segment 7 (NSP3), the only segment where we observed no recombination events (Table 2; Supplementary Table 1). A previous study reported intergenotypic recombination events in segment 6 (VP6), segment 8 (NSP2), and segment 10 (NSP4) (Jere, Mlera et al. 2011), so our study adds to the number of segments able to tolerate intergenotypic recombination. Interestingly, the serotype proteins, VP4 and VP7, have the most different genotypes, with 51 and 36 respectively (Steger, Boudreaux et al. 2019). Given this genetic diversity, the chances of two viruses with different G or P types coinfecting a cell is substantially higher than other segments. In addition, both VP4 and VP7 seem to be more prone to reassortment, and to tolerate more divergent genetic backgrounds or genome constellations (Martella, Ciarlet et al. 2003, Gentsch, Laird et al. 2005, McDonald, Matthijnssens et al. 2009, Patton 2012). This diversity and tolerance of many different genetic backgrounds implies that VP4 and VP7 may be more tolerant of recombination between divergent strains than the other segments. Our data seem to support this claim.

Specifically, we observed numerous instances of intergenotypic recombination in segment 9, the VP7 coding segment (Table 2; Supplementary Table 1). These events appear to be beneficial because the recombinant genotypes persisted in populations long enough for multiple samples showing the same event to be sampled (Table 2). For example, the same mosaic VP7 G6 gene (Fig. 8) was sequenced in multiple bovine strains, one isolated in 2009 (HM591496) and another in 2012 (KF170899), by two separate research groups. While still differentiable, the parents are closely related. However, in some instances, events between highly divergent genotypes seem to have been able to persist in populations. Both a 2014 Malawi isolate (MG181727) and a 2006 isolate from the United States (KC443034) showed a similar G1-G2 VP7 mosaic gene (Fig. 8). The fact that these two G genotypes are highly divergent from one another and were identified in different years in different locations by different research groups supports the contention that it is a true recombination event. Altogether, 22/24 instances of recombination in segment 9 occurred between different G serotypes (Supplementary Table 1). These examples indicate that mosaic genes formed from two divergent genotypes are relatively common and increase the diversity of circulating VP7 genotypes.

In addition, 7/16 instances of recombination in segment 4 (VP4) were intergenotypic. Recombination was observed between P4-P8, P6-P8, and P8-P14 serotypes (Supplementary Table 1). P4, P6 and P8 are all relatively closely related being in the P[II] genogroup, while P14 is in the P[III] genogroup. These putative recombination events suggest that relevant serotype diversity in human hosts is expanding. However, as P4, P6,

and P8 are also the dominant P types in human infections, there is a sampling bias towards this genogroup as the genotypes within this group are more likely to coinfect humans, so caution should be taken with this conclusion.

Segment 5 (NSP1) also showed recombination between highly divergent strains. Not only is NSP1 not strictly required for viral replication (Hua, Chen et al. 1994), it is also the least conserved of all rotavirus proteins, including even the serotype proteins VP4 and VP7 (Arnold and Patton 2011), suggesting that intergenotypic recombination disrupting the protein's amino acid sequence may be less likely to be deleterious.

Segments 7 (NSP3), 8 (NSP2), 10 (NSP4), and 11 (NSP5) all had low rates of recombination. These segments are short thus recombination is expected to be less likely, however segment 9 (VP7), one of the smallest segments, defies this pattern, having a high number of events observed. The smaller segments may also be less able to tolerate recombination events due to the important roles they play during the formation and stabilization of the supramolecular RNA complex (Fajardo, Sung et al. 2015) during rotavirus packaging and assembly (Li, Manktelow et al. 2010, Suzuki 2015, Borodavka, Dykeman et al. 2017, Fajardo, Sung et al. 2017).

Generation of Escape Mutants

Recombination involving regions encoding conserved epitopes, especially in segments that encode proteins involved in host cell attachment and entry, may provide selective advantages to rotaviruses by allowing them to evade inactivation by host-produced antibodies. These escape mutants may be generally less fit than wildtype viruses, but competitively advantaged in hosts because of a lack of host recognition. Subsequent intrahost adaptation may then select for compensatory fitness-increasing mutations allowing these strains to be competitive with circulating rotavirus strains. Many of the recombination events observed in our study appeared to generate such escape mutants. For example, we found two instances of the same segment 9 (VP7) G1-G3 recombination event (Table 2; KJ751729 and KP752817) with amino acid changes in two of four conserved epitope regions due to the recombination event, which suggests that this strain prevailed in the population because it was better able to evade antibody neutralization.

Based on the I-TASSER structural predictions, the putative recombinant VP7 proteins detected in our survey appear able to fold properly and form functional proteins despite containing amino acid sequence from different 'parental' genotypes (Fig. 6). While the secondary structure appeared slightly altered (e.g., shorter beta sheets), the recombinant VP7 proteins generally maintained their 3-dimensional shape. The selective advantage from swapping epitopes may outweigh any potential decrease in protein stability resulting from recombination.

We also identified many recombination events involving segment 4 (VP4). In order to infect cells, VP4 must be proteolytically cleaved to produce VP5* and VP8* (Arias, Romero et al. 1996). Most of the segment 4 recombination events involved the spike head of the VP8* protein or the spike body/stalk region of the VP5* protein (antigen domain). Escape mutant studies (Zhou, Burns et al. 1994, Ludert, Ruiz et al. 2002, Aoki, Settembre et al. 2009, Nair, Feng et al. 2017) for VP4 show the VP8* spike head recognizes histo-blood group antigens, which is one of rotavirus's main host range expansion barriers (Huang, Xia et al. 2012, Hu, Sankaran et al. 2018, Lee, Dickson et al. 2018). VP5* mediates membrane penetration during cell entry (Yoder and Dormitzer 2006). VP4 recombinants therefore may help the virus expand host range and aid in immune evasion.

Segment 6 (VP6) also showed recombination events resulting in substantial amino acid changes. VP6 is a more conserved protein, but also an antigenic protein that interacts with naïve B cells (Parez, Garbarg-Chenon et al. 2004). This feature suggests that there may be selection for VP6 escape mutants to evade host immune responses. Structure analyses of VP6 indicated that it is relatively conserved across genotypes (Jiang, Tsunemitsu et al. 1992, Tang, Gilbert et al. 1997, Charpilienne, Lepault et al. 2002), which may explain why VP6 seems to have more frequent intergenotypic recombination. Conserved epitopes in VP6 exist around amino acid positions 197 to 214, and 308 to 316 (Aiyegbo, Eli et al. 2014).

Recombination in Other dsRNA Viruses

Recombination has had a significant impact on the diversity of other dsRNA reoviruses (He, Ding et al. 2010). One study of 692 complete bluetongue virus segments found evidence for at least 11 unique recombinant genotypes (1.6%) (He, Ding et al. 2010). The case for recombination among bluetongue viruses is strengthened by the fact that viruses containing the same (or similar) recombinant segments were isolated by different research groups in different countries at different times, indicating that the recombinant viruses persisted and spread following the recombination event (Carpi, Holmes et al. 2010, He, Ding et al. 2010). Another study found multiple possible instances of recombination in genome segment 8 (encoding NS2) of the epizootic hemorrhagic disease virus, a reovirus similar to bluetongue virus (Anthony, Maan et al. 2009). Several studies have reported recombination among the dsRNA rice black-streaked dwarf virus, which is also a member of the *Reoviridae* family, but infects plants (Li, Xia et al. 2013, Yin, Zheng et al. 2013). Putative recombinants were identified in six of the ten Southern rice black-streaked dwarf virus segments (Li, Xia et al. 2013, Yin, Zheng et al. 2013). Finally, intragenic recombination was observed in multiple isolates of the African horse sickness virus, an *Oribivirus* of the family *Reoviridae* (Ngoveni, van Schalkwyk et al. 2019). At least one of these events appeared in multiple subsequent lineages (Ngoveni, van Schalkwyk et al. 2019).

In study of the family *Birnaviridae*, 1,881 sequences were analyzed for evidence of recombination (Hon, Lam et al. 2008). While no interspecies recombination was observed, at least eight putative instances of intraspecies recombination were observed among the infectious bursal disease viruses and the aquabirnaviruses (Hon, Lam et al. 2008). Subsequent studies focusing on the infectious bursal disease viruses supported these results, and identified additional potential recombination events (He, Ma et al. 2009, Jackwood 2012, Vukea, Willows-Munro et al. 2014). We note that birnaviruses' genetic material is in a complex with ribonucleoprotein, while the genetic material of *Reoviridae* members is free in the virion, which could be a factor in differing rates of recombination across these dsRNA viruses.

Recombination has also been observed in dsRNA mycoviruses, including in the *Partitiviridae* (Botella, Tuomivirta et al. 2015) and the *Hypoviridae* (Carbone, Liu et al. 2004, Linder-Basso, Dynek et al. 2005, Feau, Dutech et al. 2014) and the *Totiviridae* (Voth, Mairura et al. 2006). Recombination in Gammapartititvirus, which infects the fungus *Gremmeniella abietina*, may have permitted the virus to cross species borders (Botella, Tuomivirta et al. 2015). In cryphonectria hypovirus 1, which infects chestnut blight, recombination was implicated in the spread of the virus in Europe (Feau, Dutech et al. 2014). Collectively, these studies, and those

of other dsRNA families, suggest that not only is recombination possible, but also significantly impacts virus evolution. There is little doubt that this conclusion will be strengthened as more dsRNA viruses are discovered and/or sequenced.

Possible Mechanism of Recombination in Rotavirus

The precise mechanism for how rotavirus recombination occurs is unknown, but inferences can be made because many of the details regarding rotavirus replication and packaging have been resolved (McDonald and Patton 2011, Borodavka, Desselberger et al. 2018). The most-accepted hypothesis is that recombination takes place when the rotavirus +ssRNA is replicated after being packaged in the nucleocapsid (Esona, Roy et al. 2017, Jing, Zhang et al. 2018). For packaging and replication to occur, the eleven +ssRNA segments must join a protein complex consisting of the VP1 polymerase and the VP3 capping enzyme. Secondary RNA structures in the non-translated terminal regions (NTRs) aid in the formation of this supramolecular RNA complex (Fajardo, Sung et al. 2015, Borodavka, Dykeman et al. 2017) and determine whether the segments are packaged (Li, Manktelow et al. 2010, Suzuki 2015). Perhaps recombination occurs when multiple homologous RNA strands are joined in the same complex, allowing the homologous NTRs to partially hybridize. In this scenario, the VP1 polymerase replicates part of one strand before switching to the other, thus producing a recombined segment. This conjecture is supported by the fact that recombination tends to occur in segment regions where self-hybridization forms three-dimensional structures. Moreover, rotavirus do not seem constrained from packaging extra genetic material (Desselberger 1996). A similar form of template switching is seen in poliovirus, an ssRNA virus, which exhibits high rates of recombination, although the precise mechanism may be different in that case insofar as in poliovirus, the polymerase may be stalled due to a hairpin or other secondary structure, and switches to a different template (Tolskaya, Romanova et al. 1987). Further study is needed to determine the precise mechanism of recombination in rotavirus.

References

Abdel-Haq, N. M., R. A. Thomas, B. I. Asmar, V. Zacharova and W. D. Lyman (2003). "Increased prevalence of G1P[4] genotype among children with rotavirus-associated gastroenteritis in metropolitan Detroit." J Clin Microbiol **41**(6): 2680-2682.

Aida, S., S. Nahar, S. K. Paul, M. A. Hossain, M. R. Kabir, S. R. Sarkar, S. Ahmed, S. Ghosh, N. Urushibara, M. Kawaguchiya, M. S. Aung, A. Sumi and N. Kobayashi (2016). "Whole genomic analysis of G2P[4] human Rotaviruses in Mymensingh, north-central Bangladesh." Heliyon **2**(9): e00168-e00168.

Aiyegbo, M. S., I. M. Eli, B. W. Spiller, D. R. Williams, R. Kim, D. E. Lee, T. Liu, S. Li, P. L. Stewart and J. E. Crowe, Jr. (2014). "Differential accessibility of a rotavirus VP6 epitope in trimers comprising type I, II, or III channels as revealed by binding of a human rotavirus VP6-specific antibody." J Virol **88**(1): 469-476.

Anaya-Molina, Y., S. I. De La Cruz Hernández, A. E. Andrés-Dionicio, H. L. Terán-Vega, H. Méndez-Pérez, G. Castro-Escarpulli and H. García-Lozano (2018). "A one-step real-time RT-PCR helps to identify mixed rotavirus infections in Mexico." Diagnostic Microbiology and Infectious Disease **92**(4): 288-293.

Anthony, S. J., N. Maan, S. Maan, G. Sutton, H. Attoui and P. P. C. Mertens (2009). "Genetic and phylogenetic analysis of the non-structural proteins NS1, NS2 and NS3 of epizootic haemorrhagic disease virus (EHDV)." Virus Research **145**(2): 211-219.

Aoki, S. T., E. C. Settembre, S. D. Trask, H. B. Greenberg, S. C. Harrison and P. R. Dormitzer (2009). "Structure of rotavirus outer-layer protein VP7 bound with a neutralizing Fab." Science **324**(5933): 1444-1447.

Arias, C. F., P. Romero, V. Alvarez and S. Lopez (1996). "Trypsin activation pathway of rotavirus infectivity." J Virol **70**(9): 5832-5839.

Arnold, M. M. and J. T. Patton (2011). "Diversity of interferon antagonist activities mediated by NSP1 proteins of different rotavirus strains." J Virol **85**(5): 1970-1979.

Banyai, K., G. Kemenesi, I. Budinski, F. Foldes, B. Zana, S. Marton, R. Varga-Kugler, M. Oldal, K. Kurucz and F. Jakab (2017). "Candidate new rotavirus species in Schreiber's bats, Serbia." Infect Genet Evol **48**: 19-26.

Bernhart, S. H., I. L. Hofacker, S. Will, A. R. Gruber and P. F. Stadler (2008). "RNAalifold: improved consensus structure prediction for RNA alignments." BMC Bioinformatics **9**: 474.

Bertrand, Y., M. Töpel, A. Elväng, W. Melik and M. Johansson (2012). "First Dating of a Recombination Event in Mammalian Tick-Borne Flaviviruses." PLOS ONE **7**(2): e31981.

Bertrand, Y. J. K., M. Johansson and P. Norberg (2016). "Revisiting Recombination Signal in the Tick-Borne Encephalitis Virus: A Simulation Approach." PLOS ONE **11**(10): e0164435.

Boni, M. F., M. D. de Jong, H. R. van Doorn and E. C. Holmes (2010). "Guidelines for identifying homologous recombination events in influenza A virus." PLoS One **5**(5): e10434.

Boni, M. F., G. J. D. Smith, E. C. Holmes and D. Vijaykrishna (2012). "No evidence for intra-segment recombination of 2009 H1N1 influenza virus in swine." Gene **494**(2): 242-245.

Boni, M. F., Y. Zhou, J. K. Taubenberger and E. C. Holmes (2008). "Homologous Recombination Is Very Rare or Absent in Human Influenza A Virus." Journal of Virology **82**(10): 4807.

Borodavka, A., U. Desselberger and J. T. Patton (2018). "Genome packaging in multi-segmented dsRNA viruses: distinct mechanisms with similar outcomes." Current Opinion in Virology **33**: 106-112.

Borodavka, A., E. C. Dykeman, W. Schrimpf and D. C. Lamb (2017). "Protein-mediated RNA folding governs sequence-specific interactions between rotavirus genome segments." Elife **6**.

Botella, L., T. T. Tuomivirta, J. Hantula, J. J. Diez and L. Jankovsky (2015). "The European race of Gremmeniella abietina hosts a single species of Gammapartitivirus showing a global distribution and possible recombinant events in its history." Fungal Biology **119**(2): 125-135.

Bwogi, J., K. C. Jere, C. Karamagi, D. K. Byarugaba, P. Namuwulya, F. N. Baliraine, U. Desselberger and M. Iturriza-Gomara (2017). "Whole genome analysis of selected human and animal rotaviruses identified in Uganda from 2012 to 2014 reveals complex genome reassortment events between human, bovine, caprine and porcine strains." PLoS One **12**(6): e0178855.

Cao, D., M. Barro and Y. Hoshino (2008). "Porcine rotavirus bearing an aberrant gene stemming from an intergenic recombination of the NSP2 and NSP5 genes is defective and interfering." Journal of virology **82**(12): 6073-6077.

Carbone, I., Y. C. Liu, B. I. Hillman and M. G. Milgroom (2004). "Recombination and migration of Cryphonectria hypovirus 1 as inferred from gene genealogies and the coalescent." Genetics **166**(4): 1611-1629.

Carpi, G., E. C. Holmes and A. Kitchen (2010). "The Evolutionary Dynamics of Bluetongue Virus." Journal of Molecular Evolution **70**(6): 583-592.

Charpilienne, A., J. Lepault, F. Rey and J. Cohen (2002). "Identification of rotavirus VP6 residues located at the interface with VP2 that are essential for capsid assembly and transcriptase activity." Journal of virology **76**(15): 7822-7831.

Desselberger, U. (1996). "Genome rearrangements of rotaviruses." Advances in Virus Research, Vol 46 **46**: 69-95.

Desselberger, U. (2014). "Rotaviruses." Virus Research **190**: 75-96.

Donker, N. C., K. Boniface and C. D. Kirkwood (2011). "Phylogenetic analysis of rotavirus A NSP2 gene sequences and evidence of intragenic recombination." Infect Genet Evol **11**(7): 1602-1607.

Donker, N. C. and C. D. Kirkwood (2012). "Selection and evolutionary analysis in the nonstructural protein NSP2 of rotavirus A." Infection Genetics and Evolution **12**(7): 1355-1361.

Doro, R., S. L. Farkas, V. Martella and K. Banyai (2015). "Zoonotic transmission of rotavirus: surveillance and control." Expert Review of Anti-Infective Therapy **13**(11): 1337-1350.

Drummond, A. J. and A. Rambaut (2007). "BEAST: Bayesian evolutionary analysis by sampling trees." BMC Evolutionary Biology **7**(1): 214.

Edgar, R. C. (2004). "MUSCLE: multiple sequence alignment with high accuracy and high throughput." Nucleic Acids Res **32**(5): 1792-1797.

Esona, M. D., S. Roy, K. Rungsrisuriyachai, J. Sanchez, L. Vasquez, V. Gomez, L. A. Rios, M. D. Bowen and M. Vazquez (2017). "Characterization of a triple-recombinant, reassortant rotavirus strain from the Dominican Republic." Journal of General Virology **98**(2): 134-142.

Fajardo, T., Jr., P. Y. Sung and P. Roy (2015). "Disruption of Specific RNA-RNA Interactions in a Double-Stranded RNA Virus Inhibits Genome Packaging and Virus Infectivity." PLoS Pathog **11**(12): e1005321.

Fajardo, T., P. Y. Sung, C. C. Celma and P. Roy (2017). "Rotavirus Genomic RNA Complex Forms via Specific RNA-RNA Interactions: Disruption of RNA Complex Inhibits Virus Infectivity." Viruses **9**(7).

Feau, N., C. Dutech, J. Brusini, D. Rigling and C. Robin (2014). "Multiple introductions and recombination in Cryphonectria hypovirus 1: perspective for a sustainable biological control of chestnut blight." Evolutionary applications **7**(5): 580-596.

Gentsch, J. R., A. R. Laird, B. Bielfelt, D. D. Griffin, K. Banyai, M. Ramachandran, V. Jain, N. A. Cunliffe, O. Nakagomi, C. D. Kirkwood, T. K. Fischer, U. D. Parashar, J. S. Bresee, B. Jiang and R. I. Glass (2005). "Serotype diversity and reassortment between human and animal rotavirus strains: implications for rotavirus vaccine programs." J Infect Dis **192 Suppl 1**: S146-159.

664 Ghosh, A., S. Chattopadhyay, M. Chawla-Sarkar, P. Nandy and A. Nandy (2012). "In silico study of
665 rotavirus VP7 surface accessible conserved regions for antiviral drug/vaccine design." PLoS One **7**(7):
666 e40749.
667 Ghosh, S. and N. Kobayashi (2011). "Whole-genomic analysis of rotavirus strains: current status and
668 future prospects." Future Microbiology **6**(9): 1049-1065.
669 Hatcher, E. L., S. A. Zhdanov, Y. Bao, O. Blinkova, E. P. Nawrocki, Y. Ostapchuck, A. A. Schaffer and J. R.
670 Brister (2017). "Virus Variation Resource - improved response to emergent viral outbreaks." Nucleic
671 Acids Res **45**(D1): D482-d490.
672 He, C.-Q., L.-Y. Ma, D. Wang, G.-R. Li and N.-Z. Ding (2009). "Homologous recombination is apparent
673 in infectious bursal disease virus." Virology **384**(1): 51-58.
674 He, C. Q., N. Z. Ding, M. He, S. N. Li, X. M. Wang, H. B. He, X. F. Liu and H. S. Guo (2010). "Intragenic
675 recombination as a mechanism of genetic diversity in bluetongue virus." J Virol **84**(21): 11487-11495.
676 He, C. Q., G. Z. Han, D. Wang, W. Liu, G. R. Li, X. P. Liu and N. Z. Ding (2008). "Homologous
677 recombination evidence in human and swine influenza A viruses." Virology **380**(1): 12-20.
678 Hon, C. C., T. T. Lam, C. W. Yip, R. T. Wong, M. Shi, J. Jiang, F. Zeng and F. C. Leung (2008).
679 "Phylogenetic evidence for homologous recombination within the family Birnaviridae." J Gen Virol
680 **89**(Pt 12): 3156-3164.
681 Hu, L., B. Sankaran, D. R. Laucirica, K. Patil, W. Salmen, A. C. M. Ferreon, P. S. Tsoi, Y. Lasanajak, D. F.
682 Smith, S. Ramani, R. L. Atmar, M. K. Estes, J. C. Ferreon and B. V. V. Prasad (2018). "Glycan recognition
683 in globally dominant human rotaviruses." Nat Commun **9**(1): 2631.
684 Hua, J., X. Chen and J. T. Patton (1994). "Deletion mapping of the rotavirus metalloprotein NS53
685 (NSP1): the conserved cysteine-rich region is essential for virus-specific RNA binding." J Virol **68**(6):
686 3990-4000.
687 Huang, P., M. Xia, M. Tan, W. Zhong, C. Wei, L. Wang, A. Morrow and X. Jiang (2012). "Spike protein
688 VP8* of human rotavirus recognizes histo-blood group antigens in a type-specific manner." J Virol
689 **86**(9): 4833-4843.
690 Husain, M., P. Seth, L. Dar and S. Broor (1996). "Classification of rotavirus into G and P types with
691 specimens from children with acute diarrhea in New Delhi, India." Journal of Clinical Microbiology
692 **34**(6): 1592.
693 Iturriza-Gomara, M., B. Isherwood, U. Desselberger and J. Gray (2001). "Reassortment in vivo: driving
694 force for diversity of human rotavirus strains isolated in the United Kingdom between 1995 and
695 1999." J Virol **75**(8): 3696-3705.
696 Jackwood, D. J. (2012). "Molecular epidemiologic evidence of homologous recombination in
697 infectious bursal disease viruses." Avian Dis **56**(3): 574-577.
698 Jain, V., B. K. Das, M. K. Bhan, R. I. Glass and J. R. Gentsch (2001). "Great diversity of group A rotavirus
699 strains and high prevalence of mixed rotavirus infections in India." J Clin Microbiol **39**(10): 3524-3529.
700 Jere, K. C., C. Chaguza, N. Bar-Zeev, J. Lowe, C. Peno, B. Kumwenda, O. Nakagomi, J. E. Tate, U. D.
701 Parashar, R. S. Heyderman, N. French, N. A. Cunliffe, M. Iturriza-Gomara and V. Consortium (2018).
702 "Emergence of Double- and Triple-Gene Reassortant G1P 8 Rotaviruses Possessing a DS-1-Like
703 Backbone after Rotavirus Vaccine Introduction in Malawi." Journal of Virology **92**(3).
704 Jere, K. C., L. Mlera, N. A. Page, A. A. van Dijk and H. G. O'Neill (2011). "Whole genome analysis of
705 multiple rotavirus strains from a single stool specimen using sequence-independent amplification and
706 454(R) pyrosequencing reveals evidence of intergenotype genome segment recombination." Infect
707 Genet Evol **11**(8): 2072-2082.

Jiang, B., H. Tsunemitsu, J. R. Gentsch, R. I. Glass, K. Y. Green, Y. Qian and L. J. Saif (1992). "Nucleotide sequence of gene 5 encoding the inner capsid protein (VP6) of bovine group C rotavirus: comparison with corresponding genes of group C, A, and B rotaviruses." Virology **190**(1): 542-547.

Jing, Z., X. Zhang, H. Shi, J. Chen, D. Shi, H. Dong and L. Feng (2018). "A G3P 13 porcine group A rotavirus emerging in China is a reassortant and a natural recombinant in the VP4 gene." Transboundary and Emerging Diseases **65**(2): e317-e328.

Khetawat, D., P. Dutta, S. K. Bhattacharya and S. Chakrabarti (2002). "Distribution of rotavirus VP7 genotypes among children suffering from watery diarrhea in Kolkata, India." Virus Res **87**(1): 31-40.

Kirkwood, C. D. (2010). "Genetic and antigenic diversity of human rotaviruses: potential impact on vaccination programs." Journal of Infectious Diseases **202**: S43-S48.

Kiulia, N. M., I. Peenze, J. Dewar, A. Nyachieo, M. Galo, E. Omolo, A. D. Steele and J. M. Mwenda (2006). "Molecular characterisation of the rotavirus strains prevalent in Maua, Meru North, Kenya." East Afr Med J **83**(7): 360-365.

Lai, M. M. (1992). "RNA recombination in animal and plant viruses." Microbiol Rev **56**(1): 61-79.

Lee, B., D. M. Dickson, A. C. deCamp, E. Ross Colgate, S. A. Diehl, M. I. Uddin, S. Sharmin, S. Islam, T. R. Bhuiyan, M. Alam, U. Nayak, J. C. Mychaleckyj, M. Taniuchi, W. A. Petri, Jr., R. Haque, F. Qadri and B. D. Kirkpatrick (2018). "Histo-Blood Group Antigen Phenotype Determines Susceptibility to Genotype-Specific Rotavirus Infections and Impacts Measures of Rotavirus Vaccine Efficacy." J Infect Dis **217**(9): 1399-1407.

Li, W., E. Manktelow, J. C. von Kirchbach, J. R. Gog, U. Desselberger and A. M. Lever (2010). "Genomic analysis of codon, sequence and structural conservation with selective biochemical-structure mapping reveals highly conserved and dynamic structures in rotavirus RNAs with potential cis-acting functions." Nucleic Acids Res **38**(21): 7718-7735.

Li, Y., Z. Xia, J. Peng, T. Zhou and Z. Fan (2013). "Evidence of recombination and genetic diversity in southern rice black-streaked dwarf virus." Arch Virol **158**(10): 2147-2151.

Linder-Basso, D., J. N. Dynek and B. I. Hillman (2005). "Genome analysis of Cryphonectria hypovirus 4, the most common hypovirus species in North America." Virology **337**(1): 192-203.

Lorenz, R., S. H. Bernhart, C. Honer Zu Siederdissen, H. Tafer, C. Flamm, P. F. Stadler and I. L. Hofacker (2011). "ViennaRNA Package 2.0." Algorithms Mol Biol **6**: 26.

Ludert, J. E., M. C. Ruiz, C. Hidalgo and F. Liprandi (2002). "Antibodies to rotavirus outer capsid glycoprotein VP7 neutralize infectivity by inhibiting virion decapsidation." J Virol **76**(13): 6643-6651.

Lukashev, A. N. (2005). "Role of recombination in evolution of enteroviruses." Rev Med Virol **15**(3): 157-167.

Martella, V., K. Banyai, J. Matthijnssens, C. Buonavoglia and M. Ciarlet (2010). "Zoonotic aspects of rotaviruses." Veterinary Microbiology **140**(3-4): 246-255.

Martella, V., M. Ciarlet, A. Pratelli, S. Arista, V. Terio, G. Elia, A. Cavalli, M. Gentile, N. Decaro, G. Greco, M. A. Cafiero, M. Tempesta and C. Buonavoglia (2003). "Molecular analysis of the VP7, VP4, VP6, NSP4, and NSP5/6 genes of a buffalo rotavirus strain: identification of the rare P[3] rhesus rotavirus-like VP4 gene allele." Journal of clinical microbiology **41**(12): 5665-5675.

Martin, D. P., B. Murrell, M. Golden, A. Khoosal and B. Muhire (2015). "RDP4: Detection and analysis of recombination patterns in virus genomes." Virus Evol **1**(1): vev003.

Martinez-Laso, J., A. Roman, M. Rodriguez, I. Cervera, J. Head, I. Rodriguez-Avial and J. J. Picazo (2009). "Diversity of the G3 genes of human rotaviruses in isolates from Spain from 2004 to 2006: cross-species transmission and inter-genotype recombination generates alleles." J Gen Virol **90**(Pt 4): 935-943.

753 Matthijnssens, J., J. Bilcke, M. Ciarlet, V. Martella, K. Banyai, M. Rahman, M. Zeller, P. Beutels, P. Van
754 Damme and M. Van Rans (2009). "Rotavirus disease and vaccination: impact on genotype diversity."
755 Future Microbiology **4**(10): 1303-1316.
756 Matthijnssens, J., M. Ciarlet, E. Heiman, I. Arijs, T. Delbeke, S. M. McDonald, E. A. Palombo, M.
757 Iturriza-Gomara, P. Maes, J. T. Patton, M. Rahman and M. Van Ranst (2008). "Full genome-based
758 classification of rotaviruses reveals a common origin between human Wa-Like and porcine rotavirus
759 strains and human DS-1-like and bovine rotavirus strains." J Virol **82**(7): 3204-3219.
760 Matthijnssens, J., M. Ciarlet, S. M. McDonald, H. Attoui, K. Bányai, J. R. Brister, J. Buesa, M. D. Esona,
761 M. K. Estes, J. R. Gentsch, M. Iturriza-Gómara, R. Johne, C. D. Kirkwood, V. Martella, P. P. C. Mertens,
762 O. Nakagomi, V. Parreño, M. Rahman, F. M. Ruggeri, L. J. Saif, N. Santos, A. Steyer, K. Taniguchi, J. T.
763 Patton, U. Desselberger and M. Van Ranst (2011). "Uniformity of rotavirus strain nomenclature
764 proposed by the Rotavirus Classification Working Group (RCWG)." Archives of Virology **156**(8): 1397-
765 1413.
766 Matthijnssens, J., M. Ciarlet, M. Rahman, H. Attoui, K. Bányai, M. K. Estes, J. R. Gentsch, M. Iturriza-
767 Gómara, C. D. Kirkwood, V. Martella, P. P. C. Mertens, O. Nakagomi, J. T. Patton, F. M. Ruggeri, L. J.
768 Saif, N. Santos, A. Steyer, K. Taniguchi, U. Desselberger and M. Van Ranst (2008). "Recommendations
769 for the classification of group A rotaviruses using all 11 genomic RNA segments." Archives of virology
770 **153**(8): 1621-1629.
771 Matthijnssens, J., E. Heylen, M. Zeller, M. Rahman, P. Lemey and M. Van Ranst (2010). "Phylodynamic
772 Analyses of Rotavirus Genotypes G9 and G12 Underscore Their Potential for Swift Global Spread."
773 Molecular Biology and Evolution **27**(10): 2431-2436.
774 Matthijnssens, J., P. H. Otto, M. Ciarlet, U. Desselberger, M. Van Ranst and R. Johne (2012). "VP6-
775 sequence-based cutoff values as a criterion for rotavirus species demarcation." Archives of Virology
776 **157**(6): 1177-1182.
777 McDonald, S. M., J. Matthijnssens, J. K. McAllen, E. Hine, L. Overton, S. Wang, P. Lemey, M. Zeller, M.
778 Van Ranst, D. J. Spiro and J. T. Patton (2009). "Evolutionary dynamics of human rotaviruses: balancing
779 reassortment with preferred genome constellations." PLOS Pathogens **5**(10): e1000634.
780 McDonald, S. M., M. I. Nelson, P. E. Turner and J. T. Patton (2016). "Reassortment in segmented RNA
781 viruses: mechanisms and outcomes." Nature Reviews Microbiology **14**(7): 448-460.
782 McDonald, S. M. and J. T. Patton (2011). "Assortment and packaging of the segmented rotavirus
783 genome." Trends Microbiol **19**(3): 136-144.
784 Mihalov-Kovacs, E., A. Gellert, S. Marton, S. L. Farkas, E. Feher, M. Oldal, F. Jakab, V. Martella and K.
785 Banyai (2015). "Candidate new rotavirus species in sheltered dogs, Hungary." Emerg Infect Dis **21**(4):
786 660-663.
787 Minin, V. N., E. W. Bloomquist and M. A. Suchard (2008). "Smooth skyride through a rough skyline:
788 Bayesian coalescent-based inference of population dynamics." Mol Biol Evol **25**(7): 1459-1471.
789 Mwanga, M., C. A. Nyaigoti, R. Njeru, D. J. Nokes, C. Matthew, V. T. M. Phan and E. C. Holmes (2018).
790 "Unbiased whole genome deep sequencing of Rotavirus Group A positive samples from rural Kenya,
791 2012-14 reveals high frequency of coinfection and genetic reassortment." International Journal of
792 Infectious Diseases **73**: 203.
793 Mwenda, J. M., K. M. Ntoto, A. Abebe, C. Enweronu-Laryea, I. Amina, J. McHomvu, A. Kisakye, E. M.
794 Mpabalwani, I. Pazvakavambwa, G. E. Armah, L. M. Seheri, N. M. Kiulia, N. Page, M.-A. Widdowson
795 and A. Duncan Steele (2010). "Burden and Epidemiology of Rotavirus Diarrhea in Selected African
796 Countries: Preliminary Results from the African Rotavirus Surveillance Network." The Journal of
797 Infectious Diseases **202**(Supplement_1): S5-S11.

798 Nair, N., N. Feng, L. K. Blum, M. Sanyal, S. Ding, B. Jiang, A. Sen, J. M. Morton, X. S. He, W. H. Robinson
799 and H. B. Greenberg (2017). "VP4- and VP7-specific antibodies mediate heterotypic immunity to
800 rotavirus in humans." Sci Transl Med **9**(395).
801 Ngoveni, H. G., A. van Schalkwyk and J. J. O. Koekemoer (2019). "Evidence of Intragenic
802 Recombination in African Horse Sickness Virus." Viruses **11**(7).
803 Norberg, P., A. Roth and T. Bergstrom (2013). "Genetic recombination of tick-borne flaviviruses
804 among wild-type strains." Virology **440**(2): 105-116.
805 Parez, N., A. Garbarg-Chenon, C. Fourgeux, F. Le Deist, A. Servant-Delmas, A. Charpilienne, J. Cohen
806 and I. Schwartz-Cornil (2004). "The VP6 protein of rotavirus interacts with a large fraction of human
807 naive B cells via surface immunoglobulins." J Virol **78**(22): 12489-12496.
808 Parra, G. I., K. Bok, M. Martinez and J. A. Gomez (2004). "Evidence of rotavirus intragenic
809 recombination between two sublineages of the same genotype." J Gen Virol **85**(Pt 6): 1713-1716.
810 Patton, J. T. (2012). "Rotavirus diversity and evolution in the post-vaccine world." Discovery Medicine
811 **13**(68): 85-97.
812 Patton, J. T., R. Vasquez-Del Carpio, M. A. Tortorici and Z. F. Taraporewala (2007). "Coupling of
813 rotavirus genome replication and capsid assembly." Adv Virus Res **69**: 167-201.
814 Pérez-Losada, M., M. Arenas, J. C. Galán, F. Palero and F. González-Candelas (2015). "Recombination
815 in viruses: Mechanisms, methods of study, and evolutionary consequences." Infection, Genetics and
816 Evolution **30**: 296-307.
817 Phan, T. G., S. Okitsu, N. Maneekarn and H. Ushijima (2007). "Evidence of intragenic recombination in
818 G1 rotavirus VP7 genes." J Virol **81**(18): 10188-10194.
819 Phan, T. G., S. Okitsu, N. Maneekarn and H. Ushijima (2007). "Genetic heterogeneity, evolution and
820 recombination in emerging G9 rotaviruses." Infection Genetics and Evolution **7**(5): 656-663.
821 Rahman, M., J. Matthijnssens, X. Yang, T. Delbeke, I. Arijs, K. Taniguchi, M. Iturriza-Gomara, N.
822 Iftekharuddin, T. Azim and M. Van Ranst (2007). "Evolutionary history and global spread of the
823 emerging G12 human rotaviruses." Journal of Virology **81**(5): 2382-2390.
824 Rambaut, A. (2019). "Figtree v1.4.4."
825 Rambaut, A., A. J. Drummond, D. Xie, G. Baele and M. A. Suchard (2018). "Posterior Summarization in
826 Bayesian Phylogenetics Using Tracer 1.7." Systematic Biology **67**(5): 901-904.
827 Ramig, R. F. (1997). "Genetics of the rotaviruses." Annual Review of Microbiology **51**: 225-255.
828 Ramig, R. F. and R. L. Ward (1991). "Genomic segment reassortment in rotaviruses and other
829 reoviridae." Advances in Virus Research **39**: 163-207.
830 Rojas, M., H. G. Dias, J. L. S. Gonçalves, A. Manchego, R. Rosadio, D. Pezo and N. Santos (2019).
831 "Genetic diversity and zoonotic potential of rotavirus A strains in the southern Andean highlands,
832 Peru." Transboundary and Emerging Diseases **0**(0).
833 Roy, A., A. Kucukural and Y. Zhang (2010). "I-TASSER: a unified platform for automated protein
834 structure and function prediction." Nat Protoc **5**(4): 725-738.
835 Sadiq, A., N. Bostan, K. C. Yinda, S. Naseem and S. Sattar (2018). "Rotavirus: Genetics, pathogenesis
836 and vaccine advances." Reviews in Medical Virology **28**(6).
837 Sánchez-Fauquier, A., V. Montero, S. Moreno, M. Solé, J. Colomina, M. Iturriza-Gomara, A. Revilla, I.
838 Wilhelmi, J. Gray and V.-N. G. Gegavi (2006). "Human rotavirus G9 and G3 as major cause of diarrhea
839 in hospitalized children, Spain." Emerging infectious diseases **12**(10): 1536-1541.
840 Santiana, M., S. Ghosh, B. A. Ho, V. Rajasekaran, W. L. Du, Y. Mutsafi, D. A. De Jesus-Diaz, S. V.
841 Sosnovtsev, E. A. Levenson, G. I. Parra, P. M. Takvorian, A. Cali, C. Bleck, A. N. Vlasova, L. J. Saif, J. T.
842 Patton, P. Lopalco, A. Corcelli, K. Y. Green and N. Altan-Bonnet (2018). "Vesicle-Cloaked Virus Clusters
843 Are Optimal Units for Inter-organismal Viral Transmission." Cell Host Microbe **24**(2): 208-220.e208.

Schumann, T., H. Hotzel, P. Otto and R. Johne (2009). "Evidence of interspecies transmission and reassortment among avian group A rotaviruses." Virology **386**(2): 334-343.
Simon-Loriere, E. and E. C. Holmes (2011). "Why do RNA viruses recombine?" Nature Reviews Microbiology **9**(8): 617-626.
Steger, C. L., C. E. Boudreaux, L. E. LaConte, J. B. Pease and S. M. McDonald (2019). "Group A Rotavirus VP1 Polymerase and VP2 Core Shell Proteins: Intergenotypic Sequence Variation and In Vitro Functional Compatibility." Journal of Virology **93**(2): e01642-01618.
Suchard, M. A., P. Lemey, G. Baele, D. L. Ayres, A. J. Drummond and A. Rambaut (2018). "Bayesian phylogenetic and phylodynamic data integration using BEAST 1.10." Virus Evol **4**(1): vey016.
Suzuki, Y. (2015). "A candidate packaging signal of human rotavirus differentiating Wa-like and DS-1-like genomic constellations." Microbiol Immunol **59**(9): 567-571.
Suzuki, Y., T. Gojobori and O. Nakagomi (1998). "Intragenic recombinations in rotaviruses." FEBS Lett **427**(2): 183-187.
Tang, B., J. M. Gilbert, S. M. Matsui and H. B. Greenberg (1997). "Comparison of the rotavirus gene 6 from different species by sequence analysis and localization of subgroup-specific epitopes using site-directed mutagenesis." Virology **237**(1): 89-96.
Tolskaya, E. A., L. I. Romanova, V. M. Blinov, E. G. Viktorova, A. N. Sinyakov, M. S. Kolesnikova and V. I. Agol (1987). "Studies on the recombination between RNA genomes of poliovirus: the primary structure and nonrandom distribution of crossover regions in the genomes of intertypic poliovirus recombinants." Virology **161**(1): 54-61.
Varsani, A., P. Lefeuvre, P. Roumagnac and D. Martin (2018). "Notes on recombination and reassortment in multipartite/segmented viruses." Curr Opin Virol **33**: 156-166.
Vita, R., S. Mahajan, J. A. Overton, S. K. Dhanda, S. Martini, J. R. Cantrell, D. K. Wheeler, A. Sette and B. Peters (2019). "The Immune Epitope Database (IEDB): 2018 update." Nucleic Acids Res **47**(D1): D339-d343.
Voth, P. D., L. Mairura, B. E. Lockhart and G. May (2006). "Phylogeography of Ustilago maydis virus H1 in the USA and Mexico." Journal of General Virology **87**(11): 3433-3441.
Vukea, P. R., S. Willows-Munro, R. F. Horner and T. H. T. Coetzer (2014). "Phylogenetic analysis of the polyprotein coding region of an infectious South African bursal disease virus (IBDV) strain." Infection, Genetics and Evolution **21**: 279-286.
Woods, R. J. (2015). "Intrasegmental recombination does not contribute to the long-term evolution of group A rotavirus." Infection Genetics and Evolution **32**: 354-360.
Worobey, M., A. Rambaut, O. G. Pybus and D. L. Robertson (2002). "Questioning the evidence for genetic recombination in the 1918 "Spanish flu" virus." Science **296**(5566): 211 discussion 211.
Yang, J. and Y. Zhang (2015). "Protein Structure and Function Prediction Using I-TASSER." Curr Protoc Bioinformatics **52**: 5 8 1-15.
Yao, B., L. Zhang, S. Liang and C. Zhang (2012). "SVMTriP: a method to predict antigenic epitopes using support vector machine to integrate tri-peptide similarity and propensity." PLoS One **7**(9): e45152.
Yin, X., F. Q. Zheng, W. Tang, Q. Q. Zhu, X. D. Li, G. M. Zhang, H. T. Liu and B. S. Liu (2013). "Genetic structure of rice black-streaked dwarf virus populations in China." Arch Virol **158**(12): 2505-2515.
Yoder, J. D. and P. R. Dormitzer (2006). "Alternative intermolecular contacts underlie the rotavirus VP5* two- to three-fold rearrangement." The EMBO journal **25**(7): 1559-1568.
Zeldovich, K. B., P. Liu, N. Renzette, M. Foll, S. T. Pham, S. V. Venev, G. R. Gallagher, D. N. Bolon, E. A. Kurt-Jones, J. D. Jensen, D. R. Caffrey, C. A. Schiffer, T. F. Kowalik, J. P. Wang and R. W. Finberg (2015).

"Positive Selection Drives Preferred Segment Combinations during Influenza Virus Reassortment." Mol Biol Evol **32**(6): 1519-1532.
Zhang, Y. (2008). "I-TASSER server for protein 3D structure prediction." BMC Bioinformatics **9**: 40.
Zhou, Y. J., J. W. Burns, Y. Morita, T. Tanaka and M. K. Estes (1994). "Localization of rotavirus VP4 neutralization epitopes involved in antibody-induced conformational changes of virus structure." J Virol **68**(6): 3955-3964.

SUPPLEMENTARY INFORMATION

***Supplementary Table 1**. Putative recombination events identified by RDP4 for whole genome Rotavirus A sequences. A total of 117 events were identified by at least 6/7 RDP4 programs. Shaded rows indicate strongly supported events (identified by 7/7 RDP4 programs or found in multiple sequenced isolates). Events that were flagged by RDP4, but were not strongly supported are not listed here.*

Segment	Accession Number	Breakpoint Cis (Excluding Gaps)	p-Values	Representative Major Parent Sequence, Source Species, Year of Isolation, % ANI, Genogroup	Representative Minor Parent Sequence, Source Species, Year of Isolation, % ANI, Genogroup
VP1	JQ988899, *Homo sapiens*, Croatia, 2006	970 (781-986) - 1734 (1693-1751)	RDP 1.02E-43 GENECONV. 8.72E-48 BootScan 4.17E-32 MaxChi. 1.15E-17 Chimera 1.05E-17 SiScan 4.30E-19 3Seq 2.96E-09	KX632342, *Homo sapiens*, Uganda, 93.7%, R1	GQ414540, *Homo sapiens*, Germany, 2009, 98.7%, R2
VP1	KU739903, *Sus scrofa*, Taiwan, 2015	1-(747-805)	RDP 1.19E-24 GENECONV 1.41E-21 BootScan. 5.14E-21 MaxChi. 8.41E-16 Chimera 3.57E-16 SiScan. 9.64E-16 3Seq 2.83E-09	KU739900, *Sus scrofa*, Taiwan, 2015, 95.8%, R1	KU739904, *Sus scrofa*, Taiwan, 2015, 99.1%, R1
VP1	KF812721, *Homo sapiens*, South Korea, 2010	2504 (2464-2537) - 3268 (3232-116)	RDP 2.58E-22 GENECONV 2.12E-08 BootScan 4.71E-22 MaxChi 9.96E-16 Chimera 1.47E-13 SiScan 5.10E-09 3Seq 2.05E-02	JX027681, *Homo sapiens*, Australia, 2007, 98.1%, R1	JF796734, *Sus scrofa,* South Korea, 2006, 94.6%, R1
VP1	JQ069926, *Homo sapiens*, Canada, 2008	2498 (2356-2507) - 3268	RDP 9.14E-22 GENECONV 5.71E-19 BootScan 1.00E-18 MaxChi 1.30E-15 Chimera 2.51E-15 SiScan. 7.42E-23 3Seq 2.78E-25	JX195074, *Homo sapiens,* Italy, 2010, 98.1%, R1	JX027681, *Homo sapiens*, Australia, 2007, 99.6%, R1
VP1	KM454503, *Equus callabus*, USA, 1981	840 (802-951) - 3281	RDP 2.77E-15 GENECONV 1.36E-19 BootScan 4.79 E-21 MaxChi 1.55E-17 SiScan 1.27E-40 3Seq 8.22E-05	Unknown, closest = DQ838638, unknown, R2	KM454492, *Equus callabus*, United Kingdom, 1976, 99.1%, R2
VP1	KU714444, *Homo sapiens*, Malawi, 2000	1656 (1636-1673) - 1752 (1740-1766)	RDP 1.35E-18 GENECONV 1.25E-17 BootScan 3.76E-11 MaxChi 3.81E-02 Chimera 4.33E-02 3Seq 5.67E-09	JN706454, *Homo sapiens,* Thailand, 2009, 97.4%, R1	KX655451, *Homo sapiens*, Uganda, 2013, 97.9%, R2
VP1	JQ069936, *Homo sapiens*, Canada, 2009	1670 (1531-1703) - 2419 (2308-2436)	RDP 1.83E-14 GENECONV 7.68E-13 MaxChi 2.73E-08	KU248405, *Homo sapiens*, Bangladesh, 2010, 98.7%, R2	HQ657171, *Homo sapiens*, South Africa, 2009, 99.7%, R2

			Chimera 2.48E-08 SiScan 2.65E-08 3Seq 5.15E-19		
VP1	KU739903, *Sus scrofa*, Taiwan, 2015	1543 (1138-1588) - 2220 (2160-2260)	RDP 3.06E-13 GENECONV 6.19E-04 BootScan 9.40E-11 MaxChi 2.98E-08 Chimera 5.67E-08 SiScan 1.19 E-06 3Seq 2.83E-09	KU739900, *Sus scrofa*, Taiwan, 2015, 97.8%, R1	KU739904, *Sus scrofa*, Taiwan, 2015, 96.5%, R1
VP1	JQ988899, *Homo sapiens*, Croatia, 2006	222 (3094-362) - 969 (882-NA)	RDP 3.76E-12 GENECONV 4.88E-10 MaxChi 7.74E-09 Chimera 4.5E-07 SiScan 6.32E-14 3Seq 5.64E-09	KJ559215, *Homo sapiens*, Argentina, 1998, 96.8%, R1	Unknown, closest = JX195074, *Homo sapiens*, Italy, 2010, R1
VP1	KC580176, *Homo sapiens*, USA, 1988	1471 (1328-1521) - 3270	RDP 9.77E-12 GENECONV 3.81E-08 MaxChi 6.16E-12 Chimera 2.36E-04 SiScan 7.42E-23 3Seq 1.91E-20	KC580526, *Homo sapiens,* USA, 1979, 99%, R1	KC580601, *Homo sapiens,* USA, 1988, 100%, R1
VP1	JQ069918, *Homo sapiens*, Canada, 2008	604 (541-662) - 956 (889-1068)	RDP 2.42E-10 GENECONV 3.25E-08 BootScan 2.38E-09 MaxChi 5.62E-03 Chimera 5.62E-03 SiScan 1.10E-04 3Seq 1.13E-08	KJ751834, *Homo sapiens*, South Africa, 2009, 99.5%, R1	JQ069924, *Homo sapiens*, Canada, 2008, 99.7%, R1
VP1	KC579647, *Homo sapiens*, USA, 1988	35 – 1448 (1290-1498)	GENECONV 4.30E-04 BootScan 2.63E-05 MaxChi 2.34E-09 Chimera 1.41E-08 SiScan 6.55E-11 3Seq 4.34E-19	KC580601, *Homo sapiens,* USA, 1988, 100%, R1	KC579509, *Homo sapiens,* USA, 1989, 99.4%, R1
VP1	KU199270, *Homo sapiens*, Bangladesh, 2010	670 (541-711) - 1403 (1327-1445)	Flagged for 285 sequences, p-value = 3.33E-09	KX536654, *Homo sapiens*, India, 2011, 98.6%, R2	KU356640, *Homo sapiens,* Bangladesh, 2013, 100%, R2
VP1	KU356662, KU356640, *Homo sapiens*, 2013	656 (541-711) - 2661 (2600-2735)	RDP 5.87E-08 GENECONV 1.43E-04 MaxChi 9.02E-10 SiScan 6.71E-20 3Seq 6.88 E-23	KU356607, *Homo sapiens*, Bangladesh, 2013, 99.5%, R2	KC178768, *Homo sapiens*, Italy, 2007, 99.6%, R2
VP1	KU199270, *Homo sapiens*, Bangladesh, 2010	3282 (3116-50) - 1410 (1363-1478)	GENECONV 3.94E-06 BootScan 2.03E-04 MaxChi 1.20E-09 Chimera 3.36E-10 SiScan2.57E-09 3Seq 5.81E-18	JQ069920, *Homo sapiens*, Canada, 2008, 99.5%, R2	KJ751889, *Homo sapiens*, Ethiopia, 2009, 99.1%, R2
VP2	KJ753425, *Homo sapiens*, Uganda, 2011	599 (561-623) - 991 (967-1019)	RDP 6.28E-47 GENECONV 5.13E-45 BootScan 2.53E-44 MaxChi 5.39E-12 Chimera 6.10E-12 SiScan 8.38E-15 3Seq 1.96E-09	JF490148, *Homo sapiens*, Australia, 2004, 98.3%, C1	KP752972, *Homo sapiens*, Gambia, 2008, 99.7%, C2
VP2	KU714445, *Homo sapiens*, Malawi, 2000	1155(1139-1170) - 1887 (1862-1908)	RDP 2.37E-41 GENECONV 1.62E-33 BootScan 5.28E-39 MaxChi 1.26E-16 Chimera 1.42E-16 SiScan 8.61E-25 3Seq 1.96E-09	KP752983, *Homo sapiens*, South Africa, 2009, 94.3%, C1	KU714456, *Homo sapiens*, Malawi, 2000, 99.9%, C2
VP2	KX655439, *Homo sapiens*, Uganda, 2013	2713 (2672-2717) - 158 (143-171)	RDP 1.34E-25 GENECONV 9.67E-24 MaxChi 1.54E-03 Chimera 8.56E-04 SiScan 1.61E-05 3S— 2.15E--08	Unknown, closest = KX632343, *Homo sapiens*, Uganda, 2013, C2	MG181349, *Homo sapiens*, Malawi, 2002, 99.4%, C1
VP2	KJ753617, *Homo sapiens*, South Africa, 2004	548 (464-560) - 784 (754-842)	RDP 5.31E-27 GENECONV 4.03E-24 BootScan 7.13E-23	KJ752329, *Homo sapiens*, South Africa, 2003, 99.4%, C1	KX655439, *Homo sapiens*, Uganda, 2013, 98.4%, C2

			MaxChi 3.85E-05 Chimera 4.51E-05 3Seq 1.96E-09		
VP2	HM988959, *Bos taurus*, South Korea, Unknown	558 (524-586) - 2685	RDP 1.14E-21 GENECONV 2.68E-25 BootScan 2.00 E-21 MaxChi 1.29E-05 Chimera 1.11E-03 SiScan 3.88E-15 3Seq 5.94E-21	JQ069842, *Homo sapiens,* Canada, 2008, 95.2%, C1	JX971570, *Bos taurus*, South Korea, 2004, 100%, C1
VP2	MG181591, *Homo sapiens*, Malawi, 2013	1129 (1106-1140) - 1299 (1292-1318)	RDP 3.47 E-21 GENECONV 2.01E-19 BootScan 4.15E-15 MaxChi 4.04E-03 Chimera 3.95E-03 3Seq 1.96E-09	KJ753828, *Homo sapiens*, Zimbabwe, unknown, 99.1%, C2	KJ753425, *Homo sapiens*, Uganda, 2011, 99.4%, C1
VP2	KX632343, *Homo sapiens*, Uganda, 2013	2666 (2614-39) - 593 (560-612)	RDP 9.89E-21 GENECONV 2.26 E-17 BootScan 5.20E-19 MaxChi 4.65E-13 Chimera 3.18 E-13 SiSeq 2.53E-24 3Seq 1.37E-05	JN258812, *Homo sapiens*, Belgium, 2000, 91.7%, C1	KJ753402, *Homo sapiens*, South Africa, 2005, 99.5%, C2
VP2	KX632343, *Homo sapiens*, Uganda, 2013	1357 (1322-1368) - 1808 (1790-1830)	RDP 1.14E-21 GENECONV 3.44E-17 MaxChi 1.69E-11 Chimera 3.57E-10 SiScan 2.84E-14 3Seq 1.96E-09	MG181371, *Homo sapiens*, Malawi, 2002, 95.3%, C1	KJ870879, *Homo sapiens*, Democratic Republic of the Congo, 99.3%, C2
VP2	KY055428, *Capra aegagrus*, Uganda, 2014	983 (960-1009) - 1238 (1194-1243)	RDP 1.64E-18 GENECONV 1.12E-16 BootScan 2.13E-10 MaxChi 1.67E-05 Chimera 4.73E-04 SiScan 4.35E-05 3Seq 1.96E-09	JN831232, *Bos taurus*, South Africa, 2007, 94.7%, C2	KF636257, *Bos taurus*, South Africa, 2007, 99.6%, C2
VP2	KJ870901, *Homo sapiens*, Democratic Republic of the Congo, Unknown	2330 (2304-2359) - 2648 (2589-1)	RDP 1.96E-18 GENECONV 2.99E-16 BootScan 5.51E-16 MaxChi 1.71E-03 Chimera 7.67E-04 SiScan 6.29E-06 3Seq 1.96E-09	KY055417, *Sus scrofa*, Uganda, 2016, 95%, C1	LC367260, *Homo sapiens*, Nepal, 2008, 99.4%, C1
VP2	KC257092, *Camelus dromedaries*, Sudan, 2002	2047 (2017-2102) - 733 (661-754)	RDP 2.53E-16 GENECONV 4.72E-06 BootScan 7.95E-23 MaxChi 2.68E-13 Chimera 8.40E-12 SiScan 8.51E-11 3Seq 9.20E-08	Unknown, closest = DQ480724, *Homo sapiens*, Iran, unknown, C2	FJ347123, *Lama guanicoe*, Argentina, 1998, 99.9%, C2
VP2	KX632343, *Homo sapiens*, Uganda, 2013	1962 (1932-1978) – 2133 (2099-2136)	RDP 1.44E-13 GENECONV 7.46E-10 MaxChi 3.26E-06 Chimera 4.13E-05 SiScan 1.49E-07 3Seq1.96E-09	JN706477, *Homo sapiens*, Thailand, 2010, 93%, C1	KX655439, *Homo sapiens*, Uganda, 2013, 97.7%, C2
VP2	KJ627064, *Homo sapiens*, Paraguay, 2002	2675 (2615-95) - 409 (370-449)	RDP 7.01E-06 GENECONV 2.53E-03 BootScan 1.26E-04 MaxChi 4.49E-02 Chimera 3.89E-02 SiScan 1.20E-02 3Seq 9.21E-04	KJ752074, *Homo sapiens*, South Africa, 2005, 98.5%, C1	KJ752859, *Homo sapiens*, Zimbabwe, 2011, 100%, C1
VP3	KJ412679, *Homo sapiens,* Paraguay, 2009	1 (2497-3) - 1068 (1047-1080)	RDP 1.04E-72 GENECONV 1.11E-59 BootScan 1.41E-73 MaxChi 3.58E-31 Chimera 5.31E-31 SiScan 6.77E-38 3Seq 2.83E-09	JX185760, *Homo sapiens*, Italy, 2007, 97.8%, M1	KJ412622, *Homo sapiens*, Paraguay, 2009, 99.9%, M3

VP3	KP007164, *Homo sapiens*, Philippines, 2012	968 (968-996) - 1753 (1727-1777)	RDP 1.97E-38 GENECONV 2.93E-35 BootScan 2.16E-37 MaxChi 2.45E-16 Chimera 1.76E-15 SiScan 2.85E-19 3Seq 2.83E-19	KY000551, *Homo sapiens*, Germany, 2016, 99.4%, M2	KP882081, *Homo sapiens*, Bangladesh, 2007, 99.7%, M2
VP3	KX171542, *Homo sapiens*, South Korea, 2014	1465 (1432-1538) - 2482 (2461-59)	RDP 1.40E-37 GENECONV 7.17E-32 BootScan 2.84E-35 MaxChi 2.03E-19 Chimera 3.57E-19 SiScan 3.27E-23 3Seq 2.83E-09	KJ752827, *Homo sapiens,* South Africa, 2003, 98.8%, M2	KX171538, *Homo sapiens,* South Korea, 2012, 99.7%, M2
VP3	KX171543, *Homo sapiens*, South Korea, 2014	1650 (1607-1688) - 2472 (2455-59)	RDP 5.19E-37 GENECONV 2.46E-33 BootScan 2.81E-34 MaxChi 1.95E-17 Chimera 1.05E-17 SiScan 1.55E-19 3Seq 2.83E-09	KU248374, *Homo sapiens*, Bangladesh, 2010, 99.1%, M2	KC443523, *Homo sapiens*, Australia, 2007, 99.6%, M2
VP3	AB779630, *Sus scrofa,* Thailand, 2008	1590 (1578-1645) - 90 (2490-96)	RDP 3.19E-33 GENECONV 1.69E-25 BootScan 2.39E-31 MaxChi 2.05E-16 Chimera 3.42E-15 SiScan 9.38E-25 3Seq 1.42E-24	MG781054, *Sus scrofa*, 2010-2011, Thailand, 92.7%, M1	AB779632, *Sus scrofa*, Thailand, 2009, 99.9%, M1
VP3	MG181592, *Homo sapiens*, Malawi, 2013	2334 (2318-2349) - 196 (150-204)	RDP 1.09E-32 GENECONV 6.85E-18 BootScan 5.72E-27 MaxChi 6.16E-12 Chimera 9.20E-12 SiScan 3.92E-10 3Seq 3.54E-27	KC442894, *Homo sapiens*, USA, 2008, 96.4%, M2	KT919912, *Homo sapiens*, USA, 2013, 99%, M1
VP3	JN013991, *Homo sapiens*, South Africa, 2008	82 (2550-99) - 260 (253-268)	RDP 1.69E-29 GENECONV 8.98 E-27 BootScan 1.24E-17 MaxChi 9.47E-06 Chimera 1.58E-05 SiScan 1.76E-02 3Seq 5.67E-09	KJ752816, *Homo sapiens*, South Africa, 2011, 97.4%, M1	KP883027, *Homo sapiens*, Mali, 2008, 99.4%, M2
VP3	KU356576, *Homo sapiens*, Bangladesh, 2010	844 (815-855) - 1194 (1142-1219)	RDP 4.55E-24 GENECONV 1.69E-21 BootScan 3.82E-20 MaxChi 1.89E-09 Chimera 1.77E-09 SiSeq 1.18E-07 3Seq 2.83E-09	KC178787, *Homo sapiens*, Italy, 2008, 97.4%, M2	KP882081, *Homo sapiens*, Bangladesh, 2007, 100%, M2
VP3	JQ0692727, *Homo sapiens*, Canada, 2007	51 (2482-59) - 845 (817-932)	RDP 4.27E-23 GENECONV 9.70E-19 BootScan 6.96E-18 MaxChi 8.76E-14 Chimera 4.71E-14 SiScan 2.58E-17 3Seq 3.98E-35	JQ069748, *Homo sapiens*, Canada, 2008, 99.1%, M1	JQ069762, *Homo sapiens*, Canada, 2008, 99.7%, M1
VP3	JQ069754, *Homo sapiens*, Canada, 2008	835 (811-879) - 1621 (1591-1631)	RDP 6.24E-20 GENECONV 4.13E-17 BootScan 4.05E-17 MaxChi 1.69E-09 Chimera 1.31E-09 SiScan 1.91E-10 3Seq 1.71E-27	KJ627117, *Homo sapiens,* Paraguay, 1999, 99%, M1	KP645258, *Homo sapiens*, Australia, 2010, 99.7%, M1
VP3	MG181592, *Homo sapiens*, Malawi, 2013	1736 (1712-1755) - 1941 (1889-1953)	RDP 2.97E-19 GENECONV 7.80E-18 BootScan 5.65E-15 MaxChi 5.47E-04 Chimera 5.27E-04 SiSeq 9.43E-07 3Seq 2.83E-09	KC178787, *Homo sapiens,* Italy, 2008, 97%, M2	LC374087, *Homo sapiens,* Nepal, 2009, 100%, M1

VP3	KJ753665, *Homo sapiens,* South Africa, 2004	2158 (2127-2201) - 2517 (2447-64)	Flagged in 107, KA p-value= 2.23E-18, Global p-value 5.69E-11	KJ753481, *Homo sapiens*, Ethiopia, 2012, 94.9%, M1	KY055418, *Sus scrofa,* Uganda, 2016, 98.6%, M1
VP3	AB374145, *Bos taurus*, Japan, Unknown	810 (765-875) - 1544 (1486-1639)	RDP 1.85E-08 GENECONV 1.83E-04 BootScan 3.64E-05 MaxChi 1.68E-06 Chimera 3.72E-06 SiScan 2.14E-07 3Seq 4.41E-10	LC340015, *Homo sapiens*, Japan, 2014, 95.5%, M2	KJ411434, *Homo sapiens,* USA, 2012, 97.4%, M2
VP3	KJ753665, *Homo sapiens,* South Africa, 2004	1212 (1140-1312) - 1732 (1632-1801)	RDP 3.84E-07 GENECONV 3.50E-05 BootScan 1.92E-05 MaxChi 2.67E-05 Chimera 1.59E-05 SiScan 3.24E-09 3Seq 2.08E-04	HQ392255, *Homo sapiens*, Belgium, 2008, 96.2%, M1	KX778614, *Homo sapiens*, Dominican Republic of the Congo, 2013, 99.4%, M1
VP3	KJ753665, *Homo sapiens*, South Africa, 2004	580 (498-612) - 922 (831-964)	GENECONV 7.32E-11 BootScan 1.64E-09 MaxChi 3.90E-05 Chimera 3.85E-06 SiScan 9.81E-09 3Seq 7.82E-20	KP752825, *Homo sapiens,* South Africa, 2002, 99.6%, M1	JQ069760, *Homo sapiens*, Canada, 2008, 99.7%, M1
VP3	KX655453, *Homo sapiens*, Uganda, 2013	1258 (872-1389) - 1798 (1662-1917)	Flagged in 551 sequences, Global p-value= 1.78E-12	KP882576, *Homo sapiens*, Ghana, 2009, 94.9%, M2	KU714446, *Homo sapiens*, Malawi, 2000, 96.7%, M2
VP4	KX655509, *Homo sapiens*, Uganda, 2013	321 (308-323) - 683 (616-634) VP8* domain	RDP 2.16E-54 GENECONV 1.17E052 BootScan 1.59E-51 MaxChi 7.47E-19 Chimera 1.44E-18 SiScan 8.23E-23 3Seq 2.07E-09	KP902549, *Homo sapiens,* South Africa, 2003, 99.3%, P8	KJ52687, *Homo sapiens*, South Africa, 2000, 99.3%, P8
VP4	KX655487, *Homo sapiens*, Uganda, 2013	334(326-347) - 682(670-698) VP8* domain	RDP 1.06E-55 GENECONV 5.94E-51 BootScan 1.77E-50 MaxChi 4.55E-19 Chimera 5.96E-19 SiScan 1.60E-17 3Seq 2.07E-09	KX646644, H*omo sapiens*, India, 2012, 96.6%, P6	MG181340, *Homo sapiens*, Malawi, 2002, 99.7%, P8
VP4	MG181725, *Homo sapiens*, Malawi, 2014	374 (367-382) - 542 (526-553) VP8* domain	GENECONV 5.45E-46 BootScan 2.45E-41 MaxChi 4.02E-11 Chimera 3.97E-11 SiScan 2.83E-13 3Seq 2.07E-09	MG181758, *Homo sapiens*, Malawi, 2014, 99.2%, P8	MG181890, *Homo sapiens*, Malawi, 2012, 100%, P4
VP4	KU714447, *Homo sapiens*, Malawi, 2000	1380 (1378-1381) - 1562 (1543-1571)	RDP 1.47E-39 GENECONV 4.07E-38 BootScan 104E-29 MaxChi 1.24E-07 Chimera 3.25E-07 SiScan 7.45E-12 3Seq 4.14E-09	GQ869840, *Homo sapiens*, Malawi, 2000, P8	KU714458, *Homo sapiens,* Malawi, 2000, 99.5%, P14
VP4	KX655441, *Homo sapiens*, Uganda, 2013	374 (357-382)-484 (475-488) VP8* domain	RDP 5.41E-34 GENECONV 1.32E-31 BootScan2.38E-30 MaxChi 1.11E-05 Chimera 6.90E-06 SiScan 4.86E-10 3Seq 2.07E-09	LC260226, *Homo sapiens*, 2015-2016, Indonesia, 99.2%, P6	JQ069692, *Homo sapiens*, Canada, 2009, 99.1%, P8
VP4	MG181637, *Homo sapiens,* Malawi, 2013	350 (325-368) - 459 (464-466) VP8* domain	GENECONV 5.13E-28 BootScan 5.75E-15 MaxChi 2.13E-04 Chimera 1.00E-04 SiScan 4.71E-05 3Seq 4.14E-09	MG181758, *Homo sapiens*, Malawi, 2014, 99.5%, P8	KJ870892, *Homo sapiens*, Democratic Republic of the Congo, 2007-2010, 95.5%, P6
VP4	JQ069674, *Homo sapiens,* Canada, 2008	1568 (1541-1574) - 2329 (2251-101)	RDP 1.59E-23 GENECONV 2.53E-21 BootScan 1.59E-23 MaxChi 2.96E-12 Chimera 2.13E-12 SiScan 7.86E-14	HQ392253, *Homo sapiens*, Belgium, 2008, 99.5%, P8	HM773714, *Homo sapiens*, USA, 2008, 99.5%, P8

			3Seq 1.44E-35		
VP4	KC579762, *Homo sapiens*, USA, 1991	1073 (1039-1124) - 2332 (2269-8)	RDP 4.67E-23 GENECONV 4.72E-17 BootScan 8.46E-23 MaxChi 1.99E-14 Chimera 1.76E-11 SiScan 7.07E-25 3Seq 4.04E-40	HQ392253, *Homo sapiens*, Belgium, 2008, 98.7%, P8	FJ947895, *Homo sapiens*, USA, 1991, 99.9%, P8
VP4	MG181659, *Homo sapiens*, Malawi, 2013	1116 (1064-1146) - 1462 (1402-1501)	RDP 6.53E-11 GENECONV 2.20E-09 BootScan 1.08E-09 MaxChi 1.781E-05 Chimera 1.74E-05 SiScan 5.94E-06	MG181725, *Homo sapiens*, Malawi, 2013, 98.1%, P8	KJ752208, *Homo sapiens*, South Africa, 2012, 98.3%, P4
VP4	JF490554, *Homo sapiens*, Australia, 2005	462 (397-482) - 683 (637-722)	RDP 2.17E-10 GENECONV 8.75E-09 BootScan 1.89E-10 MaxChi 3.26E-04 Chimera 1.04E-03 SiScan 1.14E-04 3Seq 4.14E-09	KJ751716, *Homo sapiens,* Gambia, 2010, 98.4%, P8	JQ069674, *Homo sapiens*, Canada, 2008, 99.5%, P8
VP4	AB008291, *Homo sapiens,* 1995	2291 (2223-71) - 807 (762-849)	RDP 1.02E-03 BootScan 4.42E-02 MaxChi 5.00E-05 Chimera 1.32E-04 SiScan 1.51E-05 3Seq 1.66E-08	AB039939, *Homo sapiens*, Japan, 1990, 98.6%, P8	AB008277, *Homo sapiens*, China, 1992, 98.9%, P8
VP6	KJ482497, *Sus scrofa*, Brazil, 2013	589 (584-605) - 801 (790 – 809)	RDP 1.81E-25 GENECOV 7.17E-23 Bootscan 7.09E018 MaxChi 2.98E-10 SiScan 2.41E-11 3Seq 1.41E-09	DQ119822, *Sus scrofa,* China, unknown, 98.1%, I2	KJ482491, *Sus scrofa*, Brazil, 2013, 100%, I5
VP6	KX632346, *Homo sapiens*, Uganda, 2013	1269 (1250-1272) - 56 (1333-103)	RDP 7.77E-19 GENECONV 1.33E-17 Bootscan 7.27E-09 MaxChi 2.1E-02 Chimera 3.24E-03 SiScan 1.02E-07 3Seq 3.06E-11	KU714448, *Homo sapiens*, Malawi, 2000, 92.7%, I1	KX655455, *Homo sapiens*, Uganda, 2013, 96.5%, I2
VP6	JN014005, *Homo sapiens*, South Africa, 2008	160 (33-220 - 384 (379-451)	RDP 1.98E-18 GENECONV 6.96E-18 BootScan 4.63E-16 MaxChi 1.00E-06 Chimera 2.77E-07 3Seq 1.41E-09	JN706549, *Homo sapiens*, Thailand, 2010, 97.8%, I1	KJ752622, *Homo sapiens, Senegal*, 2009, 96.4%, I2
VP6	JX040423, *Homo sapiens*, India, 2009	1177(1143-1181) - 160(140-176)	RDP 1.30E-15 GENECONV 4.97E-09 BootScan 1.95E-11 MaxChi 4.38E-11 Chimera 9.18E-12 SiScan 7.20E-15 3Seq 2.82E-09	KF740531, *Homo sapiens*, India, 2009, I12	Unknown, closest = KC579918, *Homo sapiens*, USA, 1976), I1
VP6	JN014003, *Homo sapiens,* South Africa, 2008	202 (1333-208) - 384(354-421)	RDP 6.30E-15 GENECONV 2.39E-15 BootScan 1.04E-12 MaxChi 3.76E-05 Chimera 3.02E-05 SiScan 4.51E-05 3Seq 1.41E-09	KP752725, *Homo sapiens*, Swaziland, 2010, 95.5%, I2	JX027952, *Homo sapiens*, Australia, 2010, 96.7%, I1
VP6	KU714448, *Homo sapiens*, Malawi, 2000	653(635- 664) - 831(818-846)	RDP 1.24E-12 GENECONV 7.55E-10 BootScan 5.50E-07 MaxChi 1.15E-05 Chimera 3.38E-05 SiScan 1.38E-04 3Seq 1.41E-09	JN014005, *Homo sapiens*, South Africa, 2008, 95.9%, I1	KX655455, *Homo sapiens*, Uganda, 2013, 99.4%, I2
VP6	KU714448, *Homo sapiens*, Malawi, 2000	317 (290-333) - 491 (474-507)	RDP 3.94E-15 GENECONV 9.37E-14 BootScan 2.42E-13 MaxChi 2.80E Chimera 2.58E-05	KX638567, *Homo sapiens*, India, 2010, 96.6%, I1	GU984758, *Bos taurus*, India, 2007, 98.9%, I2

			SiScan 1.73E-07 3Seq 1.41E-09		
VP6	HQ11009, *Homo sapiens*, Belgium, 2007, 98.5%	754 (697-775) - 1357 (1329-32)	GENECONV 2.23E-05 BootScan 1.61E-03 MaxChi 3.32E-11 Chimera 1.08E-10 SiScan 5.16E-14 3Seq 2.54E-19	MF469405, *Homo sapiens*, USA, 2015, 99.3%, I1	HQ392161, *Homo sapiens*, Belgium, 2007, 98.5%, I1
VP6	FJ685614, *Homo sapiens*, India, 1992	698(672-712) - 1357 (1231-70)	RDP 1.72E-08 GENECONV 1.61E-07 BootScan 2.85E-08 MaxChi 1.40E-09 Chimera 2.14E-09 SiScan 4.04E-11 3Seq 1.54E-23	KX638599, *Homo sapiens*, India, 2010, 99.4%, I1	KX632291, *Homo sapiens*, Uganda, 2013, 99.1%, I1
VP6	KJ753780, *Homo sapiens*, South Africa, 2004	513 (463-560) - 1008 (952-1031)	GENECONV 1.89E-05 BootScan 2.60E-05 MaxChi 9.01E-09 Chimera 1.46E-08 SiScan 1.38E-09 3Seq 1.30E-19	JN258839, *Homo sapiens*, Belgium, 2001, 99.6%, I1	LC056797, *Homo sapiens*, Vietnam, 2007, 98.8%, I1
VP6	HM988972, *Bos taurus*, South Korea, Unknown	751 (340-811) - 1113 (1080-1132)	RDP 2.08E-08 GENECONV 1.92E-08 BootScan 2.91E-08 MaxChi 1.45E-05 Chimera 2.41E-05 SiScan 3.56E-05 3Seq 5.55E-05	Unknown, closest = MH238302, *Sus scrofa*, Spain, 2017, I5	MH423866, *Sus scrofa*, China, 2016, 99.4%, I5
VP7	AB158431, *Bos taurus,* Japan, 2000	901 (868-907)-1051 (1037-80)	RDP 3.71E-16 GENECONV 1.25E-13 MaxChi 6.99E-07 Chimera 3.69E-05 SiScan 8.07E-10 3Seq 4.95E-10	AB077053, *Bos taurus*, Japan, 1995-1996, 95.9%, G8	U50332, *Bos taurus,* USA, 1991, 97.2%, G6
VP7	HM591496, *Bos taurus*, India, 2009 KF170899, *Bos taurus*, India, 2012	1048 (1032-128) - 481 (448-506)	RDP 2.78E-05 GENECONV 4.77 E-04 BootScan 4.86E-04 MaxChi 1.02E-03 Chimera 3.78E-05 SiSeq 7.21E-09 3Seq 3.90E-08	EF199501, *Bos taurus,* India, 2001-2005, 96.6%, G6	JX442784, *Bos taurus*, India, 2010, 100%, G6
VP7	D86274, *Homo sapiens,* 1990	353 (338-368) - 745 (730-756)	RDP 1.73E-18 GENECONV 1.43E-16 BootScan 2.50E-14 MaxChi 3.26E-13 Chimera 6.54E-13 SiScan 2.47E-10 3Seq 3.55E-33	D86282, *Homo sapiens,* Japan, 1981, 98.7%, G3	KF636217, *Homo sapiens*, South Africa, 2010, 94.9%, G1
VP7	MG181727, *Homo sapiens*, Malawi, 2014	316 (1010-314) - 470 (437-476)	RDP 3.69E-17 GENECONV 1.84E-16 BootScan 8.96E-12 MaxChi 2.23E-08 Chimera 3.80E-08 SiScan 2.65E-12 3Seq 2.69E-23	JQ069508, *Homo sapiens*, Canada, 2008, 98%, G1	KJ753362, *Homo sapiens*, South Africa, 2003, 98.7%, G2
VP7	KX655511, *Homo sapiens*, Uganda, 2013	840 (823-851)-1052 (1037-79)	RDP 1.20E-16 GENECONV 3.11E-15 BootScan 2.21E-16 MaxChi 6.12E-05 Chimera 6.98E-06 SiScan 2.52E-04 3Seq 3.36E-09	EU839936, *Homo sapiens*, Bangladesh, 2005, 97.4%, G9	KX655456, *Homo sapiens*, Uganda, 2013, 100%, G8
VP7	KJ753024, *Homo sapiens*, South Africa, 2009	1013 (985-59) - 130(121-143)	RDP 1.53E-16 GENECONV 2.32E-14 BootScan 1.27E-10 MaxChi 9.65E-04 Chimera 5.96E-04 SiScan 8.42E-13 3Seq 2.38E-16	KM008672, *Homo sapiens*, India, 2010, 97.8%, G12	D16344, *Homo sapiens*, 96.5%, Japan, 1977, G1
VP7	KJ751729, *Homo sapiens*, Ethiopia, 2010	857 (833-859) - 1019 (991-51)	RDP 4.0E-15 GENECONV 1.60E-10 BootScan 1.21EE-11	KJ560447, *Homo sapiens*, USA, 2011, 99%, G3	KP882703, *Homo sapiens*, Kenya, 2009, 99.3%, G1

	KP752817, *Homo sapiens*, Togo, 2010		MaxChi 1.12E-03 Chimera 6.78E-04 SiScan 1.73E-03 3Seq 1.34E-05		
VP7	MG181661, *Homo sapiens,* Malawi, 2013	590 (582-616) - 175 (170-181)	RDP 7.82E-30 GENECONV 7.33E-23 BootScan 5.06E-31 MaxChi 3.49E-21 Chimera 1.06E-25 3Seq 2.28E-47	JQ069502, *Homo sapiens,* Canada, 2008, 96.6%, G1	MG181859, *Homo sapiens*, Malawi, 2012, 99.5%, G2
VP7	KF170899, *Bos taurus,* India, 2010	(71) - (448-506)	RDP 2.78 E-05 GENEECONV 4.77 E-04 BootScan 4.86 E-04 MaxChi 1.02 E-03 Chimaera 3.78 E-05 SiScan 7.21 E-09 3Seq 3.90 E-08	EF199501, *Bos taurus,* India, 2001-2005, 97.3%, G6	JX442784, *Bos taurus*, India, 2010, 99.5%, G6
VP7	KJ412857, *Homo sapiens,* Paraguay, 2009	772 (754-779) - 1014(988-51)	GENECONV 1.23E-19 BootScan 6.33E-20 MaxChi 2.56E-07 Chimera 4.38E-07 SiScan 2.01E-09 3Seq 3.36E-09	KJ412858, *Homo sapiens,* Paraguay, 2009, 100%, G3	KJ412802, *Homo sapiens*, Paraguay, 2009, 99.2%, G1
VP7	KC443034, *Homo sapiens,* USA, 2006 MG181727, *Homo sapiens,* Malawi, 2014	55 (994-60) - 291 (262-296)	RDP 1.66 E-30 GENECONV 5.07E-26 BootScan 2.32E-24 MaxChi 1.03E32 Chimaera 1.10E-17 3Seq 3.36E-09	GQ229044, *Homo sapiens*, India, 2005-2008, 97.4%, G2	JX411970, *Homo sapiens*, India, 2011, 98.7%, G1
VP7	MG181771, *Homo sapiens*, Malawi, 2012	715 (707-722) - 950 (921-971)	RDP 2.65E-29 GENECONV 6.45E-26 BootScan 5.84E-17 MaxChi 1.70E-11 Chimaera 2.36E-11 SiScan 4.78E-11 3Seq 3.55E-09	KU356667, *Homo sapiens*, Bangladesh, 2013, 94.9%, G2	KP222809, *Homo sapiens*, Mozambique, 2011, 99.6%, G1
VP7	KP752498, *Homo sapiens*, Togo, 2009	618 (605-641) - 1018 (1000-1020)	RDP 1.47E-28 GENECONV 4.49E-23 BootScan 2.78E-14 MaxChi 2.05E-14 Chimaera 7.10E-19 SiScan 6.78E-39	D86266, *Homo sapiens*, Japan, 1995, 95.7%, G3	MG181661, *Homo sapiens*, Malawi, 2013, 98.8%, G1
VP7	AY261339, *Homo sapiens*, South Africa	783 (774-791) - 14(1044-18)	RDP 3.82E-28 GENECONV 2.35E-25 BootScan 2.41E-27 MaxChi 5.44E-10 Chimera 2.33E-10 SiScan 3.15E-14 3Seq 3.36E-09	GU567778, *Homo sapiens*, Russia, 2003-2009, 96.9%, G2	JX458964, *Homo sapiens*, Argentina, 2001, 100%, G1
VP7	KX655489, *Homo sapiens*, Uganda, 2013	151 (132-155) - 316 (311-325)	RDP 2.14E-27 GENECONV 1.27E024 BootScan 3.15E-19 MaxChi 7.75E-09 Chimera 7.42E-09 SiScan 8.44E-20 3Seq 4.13E-03	DQ146676, *Homo sapiens*, Bangladesh, 2003, 98.1%, G12	JN232074, *Homo sapiens,* Brazil, 2004, 99.4%, G1
VP7	D86273, *Homo sapiens*, 1986	347 (339-353) - 726 (697-763)	RDP 1.70E-24 GENECONV 1.57E-22 BootScan 1.26E-17 MaxChi 7.23E-14 Chimera 1.37E-15 SiScan 1.73E-13 3Seq 6.15E-47	AF450293, *Homo sapiens*, China, Unknown, 97.4%, G3	D50121, *Homo sapiens*, 96.3%, Japan, 1992-1993, G2
VP7	KJ4122858, *Homo sapiens*, Paraguay, 2009	881 (859-914) - 1016 (991-54)	RDP 4.80E-14 GENECONV 3.04E-13 BootScan 3.81E-13 MaxChi 5.36E-03 Chimera 1.05E-02	AB585923, *Homo sapiens*, Hong Kong, 2006, 98.5%, G3	HQ425288, *Homo sapiens*, South Korea, 2004, 99.2%, G4

			SiScan 1.36E-04 3Seq 3.36E-09		
VP7	KU714449, *Homo sapiens*, Malawi, 2000	825 (795-835) - 93 (85-93)	RDP 1.04E-13 GENECONV 4.64E-09 BootScan 1.71E-09 MaxChi 1.20E-10 Chimera 9.96E-11 SiScan 3.89E-10 3Seq 7.72E-08	KM008635, *Homo sapiens*, India, 2009, 92.5%, G1	KU714460, *Homo sapiens,* Malawi, 2000, 98.2%, G6
VP7	KJ412888, *Homo sapiens*, Paraguay, 2009	873 (823-890) - 1023 (1000-81)	RDP 2.17E-12 GENECONV 7.16E-11 BootScan 3.63E-12 MaxChi 5.48E-04 Chimera 4.30E-04 SiScan 8.10E-03 3Seq 1.12E-05	D86275, *Homo sapiens*, China, 1986, 88%, G3	JF490143, *Homo sapiens*, Australia, 2004, 99.3%, G1
VP7	KX655445, *Homo sapiens*, Uganda, 2013	1042 (1006-110) - 274 (269-287)	RDP 6.32E-12 GENECONV 5.98E-10 BootScan 8.41E-08 MaxChi 2.20E-06 Chimera 3.68E-08 SiScan 3.20E-04 3Seq 8.29E-11	KJ560447, *Homo sapiens,* USA, 2011, 95.8%, G3	KJ753326, *Homo sapiens*, Kenya, unknown, 94.9%, G8
VP7	D86277, *Homo sapiens,* China, 1989	335 (323-353)- 754 (710-762)	RDP 8.20E-20 GENECONV 2.21E-15 BootScan 1.81E-10 MaxChi 1.91E-12 Chimera 1.95E-13 SiScan 3.36E-13 3Seq 7.22E-27	D86279, *Homo sapiens,* China, 1992, 89.6%, G3	KP883055, *Homo sapiens,* Mali, 2009, 95.7%, G2
VP7	AF281044, *Homo sapiens,* Ireland, 1997-1999 GQ433992, *Homo sapiens,* Ireland, Unknown	362 (346-366) - 589 (558-605)	RDP 1.32E-09 GENECONV 1.25E-02 BootScan 4.96E-05 MaxChi 2.75E-05 Chimera 1.50E-04 3Seq 3.36E-09	AY866503, *Homo sapiens*, Thailand, 1995-1997, 98.9%, G9	KM008633, *Homo sapiens,* India, 2009, 89%, G1
VP7	KU714449, *Homo sapiens*, Malawi, 2000	440 (421-446) - 604(641-704)	RDP 3.12E-10 GENECONV 7.36E-11 BootScan 1.56E-07 MaxChi 1.83E-03 Chimera 1.69E-03 3Seq 1.08E-12	JQ069503, *Homo sapiens*, Malawi, 2000, 100%, G1	KU714460, *Homo sapiens*, Malawi, 2000, 100%, G6
VP7	KX655444, *Homo sapiens*, Uganda, 2013	110 (88-114) - 191(183-197)	RDP 2.84E-08 GENECONV 3.00E-05 MaxChi3.11E-02 Chimera 3.11E-02 SiScan 1.01E-03 3Seq 8.25E-05	KC579965, *Homo sapiens*, USA, 1978, 96.2%, G3	AF254137, *Homo sapiens*, Ireland, 1997-1999, 93.9%, G1
NSP1	KP753174, *Sus scrofa,* South Africa, 2008, KJ753184, *Sus scrofa,* South Africa, 2008, KP752951, *Sus scrofa*, South Africa, 2008	1498 (1435-25) - 585(573-596)	RDP 7.45E-28 GENECONV 5.26E-27 BootScan 7.87E-25 MaxChi 8.49E-16 Chimera 5.73E-16 SiScan 9.95E-18 3Seq 1.09E-48	KP752999, *Sus scrofa*, South Africa, 2009, 99.9%, A8	KP753000, *Sus scrofa*, South Africa, 2009, 99.7%, A8
NSP1	KX655446, *Homo sapiens*, Uganda, 2013	485 (455-499)- 889 (868-914)	RDP 3.98E-25 GENECONV 2.55E-22 BootScan 2.53E-21 MaxChi 1.96E-14 Chimera 8.97E-15 SiScan 1.22E-19 3Seq 3.18E-09	LC406825, *Homo sapiens*, Kenya, 2012, 95.9%, A2	MG181277, *Homo sapiens*, Malawi, 2000, 96.5%, A1
NSP1	DQ199658, *Homo sapiens*, Australia, 2001	485 (440-517) - 942 (931-956)	RDP 2.25E-22 GENECONV 7.04E-20 BootScan 1.52E-21 MaxChi 2.09E-12 Chimera 1.10E-12 SiScan 6.14E-12 3Seq 2.61E-35	KP883160, *Homo sapiens*, Malawi, 2008, 98.1%, A1	DQ199657, *Homo sapiens,* Australia, 1997, 98.7%, A1
NSP1	KJ482257, *Sus scrofa*, Brazil, 2013	1534 (1490-44) - 888 (853-909)	RDP 3.24E-20 GENECONV 2.11E-19 BootScan 5.21E-10	KJ482252, *Sus scrofa*, Brazil, 2013, 92.9%, A8	KJ482255, *Sus scrofa*, Brazil, 2013, 99.9%, A8

			MaxChi 9.52E-18 SiScan 2.81E-21 3Seq 1.81E-29		
NSP1	KX778616, *Homo sapiens*, Dominican Republic, 2013	1147 (1127-1155) - 1462 (1433-5)	RDP 1.14E-19 GENECONV 4.51E-17 BootScan 8.47E-16 MaxChi 1.54E-11 Chimera 1.93E-12 SiScan 9.28E-13 3Seq 3.18E-09	KJ752290, *Homo sapiens*, Zambia, 2009, 96.3%, A1	KX363351, *Sus scrofa*, Vietnam, 2012, 95.9%, A8
NSP1	KJ482254, *Sus scrofa*, Brazil, 2013	534 (499-559) - 886 (849-911)	RDP 7.72E-18 GENECONV 1.84E-16 BootScan 3.89E-14 MaxChi 2.53E-10 Chimera 2.27E-10 SiScan 1.55E-08 3Seq 8.01E-16	KJ482247, *Sus scrofa*, Brazil, 2013, 100%, A8	KJ482256, *Sus scrofa*, Brazil, 2013, 100%, A8
NSP1	KX632348, *Homo sapiens*, Uganda, 2013	580 (508-605) - 844 (829-874)	RDP 1.91E-10 GENECONV 3.85E-10 BootScan 1.02E-06 MaxChi 2.32E-04 Chimera 2.29E-04 SiScan 6.75E-08 3Seq 3.18E-09	KP752785, *Homo sapiens*, Ethiopia, 2010, 94.9%, A1	KP882434, *Homo sapiens,* Ghana, 2009, 92.8%, A2
NSP1	KP752999, *Sus scrofa*, South Africa, 2009	1394 (1368-31) - 601 (552-631)	RDP 1.38E-06 BootScan 5.20E-05 MaxChi 2.04E-08 Chimera 2.74E-08 SiScan 3.04E-06 3Seq 2.78E-12	KF835942, *Homo sapiens,* Hungary, 2005, 93.9%, A8	Unknown, closest = KP753000 *Sus scrofa*, South Africa, 2009, A8
NSP1	JX040426, *Homo sapiens*, India, 2009	662 (559-677) - 842 (783-884)	RDP 8.72E-03 GENECONV 1.35E-05 BootScan 4.19E-02 MaxChi 1.57E-04 Chimera 5.50E-05 SiScan 4.50E-03 3Seq 6.62E-07	KU292525, *Homo sapiens,* India, 2014, 98.4%, A11	KP882478, *Homo sapiens*, Ghana, 2008, 95%, A11
NSP1	KP753000, *Sus scrofa*, South Africa, 2009	1389 (1359-41) - 602 (504-631)	RDP 4.27E-03 BootScan 4.30-03 MaxChi 1.12E-04 Chimera 1.52E-05 SiScan 3.90E-04 3Seq 5.58E-05	JQ309141, *Equus callabus,* United Kingdom, 1975, 87.2%, A8	KF835942, *Homo sapiens*, Hungary, 2005, 92.8%, A8
NSP1	KJ482254, *Sus scrofa,* Brazil, 2013	1534 (1461-44) – 533 (499-909)	GENECONV: 1.50E-13 BootScan: 5.96E-10 MaxChi: 3.77E-08 Chimaera: 6.43E-08 SiScan: 1.88E-11 3Seq: 1.46 E-24	KJ482247, *Sus scrofa,* Brazil, 2013, 99.1%, A8	KJ482255, *Sus scrofa,* Brazil, 2013, 100%, A8
NSP2	KJ753657, *Homo sapiens,* South Africa, 2004 KM026663, *Homo sapiens,* Brazil, 2009 KM026664, *Homo sapiens,* Brazil, 2009	(0) - (219 -278)	RDP 2.01E-03 GENECONV 1.6E-04 BootScan 4.07E-06 MaxChi 3.51E-03 Chimera 3.30E-03 SiScan 1.90E-07 3Seq 1.57E-04	KM026633, *Homo sapiens*, Brazil, 2003, 98.6%, N1	KJ918915, *Homo sapiens*, Hungary, 2012, 99.5%, N1
NSP2	MF18783, *Homo sapiens*, USA, 2011	1015 (1002-57) - 286 (273-297)	GENECONV 1.60E-14 BootScan 1.55E-14 MaxChi 6.46E-04 Chimera 3.74E-06 SiScan 4.37E-08 3Seq 5.75E-22	KJ752146, *Homo sapiens*, South Africa, 2011, 99.7%, N1	KX655480, *Homo sapiens,* Uganda, 2012, 99.3%, N2
NSP2	MF18783, *Homo sapiens*, USA, 2011	1015 (1002-57) - 286 (273-297)	GENECONV 1.60E-14 BootScan 1.55E-14 MaxChi 6.46E-04 Chimera 3.74E-06 SiScan 4.37E-08 3Seq 5.75E-22	KJ752146, *Homo sapiens*, South Africa, 2011, 99.7%, N1	KX655480, *Homo sapiens*, Uganda, 2012, 99.3%, N2
NSP2	AB779641, *Sus scrofa*, Thailand, 2008	870 (833-921) - 216 (150-396)	RDP 6.30E-05 GENECONV 4.67 E-03 BootScan 1.24 E-03	KX363374, *Sus scrofa*, Vietnam, 2012, 96.5%, N1	JF796719, *Sus scrofa*, South Korea, 2006, 100%, N1

			MaxChi 1.28 E-03 Chimaera 6.20 E-03 3Seq 1.48 E-05		
NSP4	MF58092, *Homo sapiens,* China, 2013	599 (546-616) - (745-94)	RDP 1.64 E-11 GENECONV 2.38 E-08 BootScan 1.14 E-09 MaxChi 1.01 E-09 Chimaera 4.58 E-10 SiScan 4.77 E-18 3Seq 6.43 E-21	JF813107, *Homo sapiens*, China, 2008, 97.9%, E1	MG781050, *Homo sapiens*, Thailand, 2011, 73.1%, E1
NSP4	AB361290, *Homo sapiens*, India, 2006	624 (548-635) - 726 (712-50)	RDP 1.66 E-09 GENECONV 4.38 E-08 BootScan 6.96 E-07 MaxChi 1.96 E-03 Chimaera 2.49 E-05 3Seq 1.15 E-12	AB326338, *Homo sapiens,* India, 1989, 95.8%, E2	Unknown, closest = FJ492834, *Sus scrofa*, Ireland, E9
NSP4	AB326966, *Homo sapiens*, India, 2001	605 (564-614) - 675 (670-46)	RDP 2.77 E-09 GENECONV 1.10 E-10 BootScan 2.26 E -02 MaxChi 2.54 E -05 Chimaera 1.63 E -03 3Seq 8.89 E-09	FJ685615, *Homo sapiens*, India, 1992, 98.2%, E1	Unknown, closest = MG181929, *Homo sapiens*, Malawi, 2012, E2
NSP5	M33608, *Homo sapiens,* 1993	619 (505-624) - 668 (665-182)	RDP 1.44 E -05 GENECONV 2.64 E-06 BootScan 4.1 E-05 MaxChi 4.54 E-02 Chimaera 3.70 E-02 SiScan 2.49 E-05 3Seq 6.61 E-04	MG996138, *Homo sapiens*, Singapore, 2016, 95%, H2	JQ358774, *Homo sapiens*, India, 2011, 100%, H3

Supplementary Table 2. *Amino acid changes observed in segment 9 (VP7) recombination events observed in more than one isolate. Changes occurring in predicted epitope regions are noted.*

Gene recombinant	**Accession Number**	**Position**	**Major**	**Minor**	**Epitope region?**
G6-G6	KF170899	40	M	T	-
		46	I	T	-
		48	V	T	-
		116	V	I	-
G3-G1	KJ751729	281	V	I	Yes
		303	V	I	Yes
		309	A	V	Yes
		318	N	D	
G9-G1	AF281044	135	S	C	-
		162	D	E	-
		163	R	W	-
		169	V	D	
		170	N	I	
		176	L	Q	
		180	G	E	Yes
G2-G1	KC443034	9	I	T	-

		10	F	I	-
		21	S	Y	-
		25	T	S	-
		26	I	V	-
		28	N	R	-
		29	P	I	-
		31	A	D	-
		32	P	Y	-
		35	F	Y	-
		41	I	F	-
		42	A	V	-
		43	L	A	-
		44	M	L	-
		45	S	F	-
		47	F	L	-
		48	G	T	-
		49	R	K	-
		50	T	A	-
		56	Y	N	-
		65	A	T	-
		68	T	S	-
		72	S	R	-
		73	G	E	-
		75	S	V	-

907

908

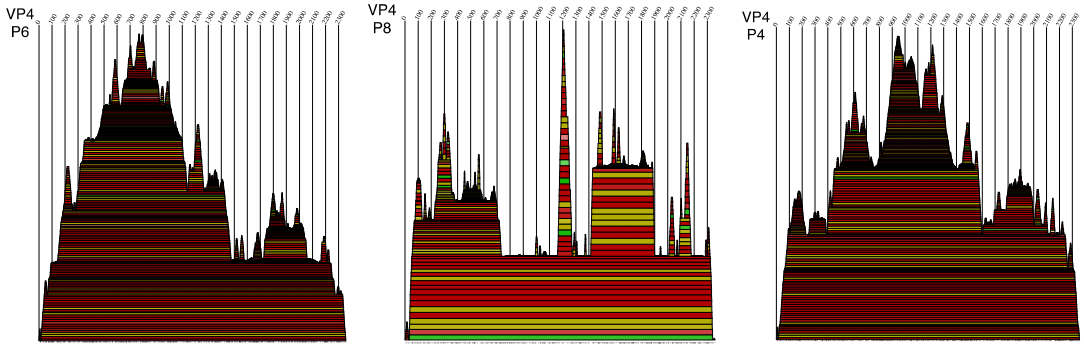

Supplementary Figure 1. *P6, P8, and P4 consensus RNA secondary structure mountain plots. Mountain plots showing consensus secondary structure of VP4 genotypes P6, P8, and P4. Lighter colors indicate lower probabilities of base-pairing. Peaks correspond to hairpin-loops, plateus to loops, and slopes to helices. Plot was generated using RNAalifold in the ViennaRNA package.*

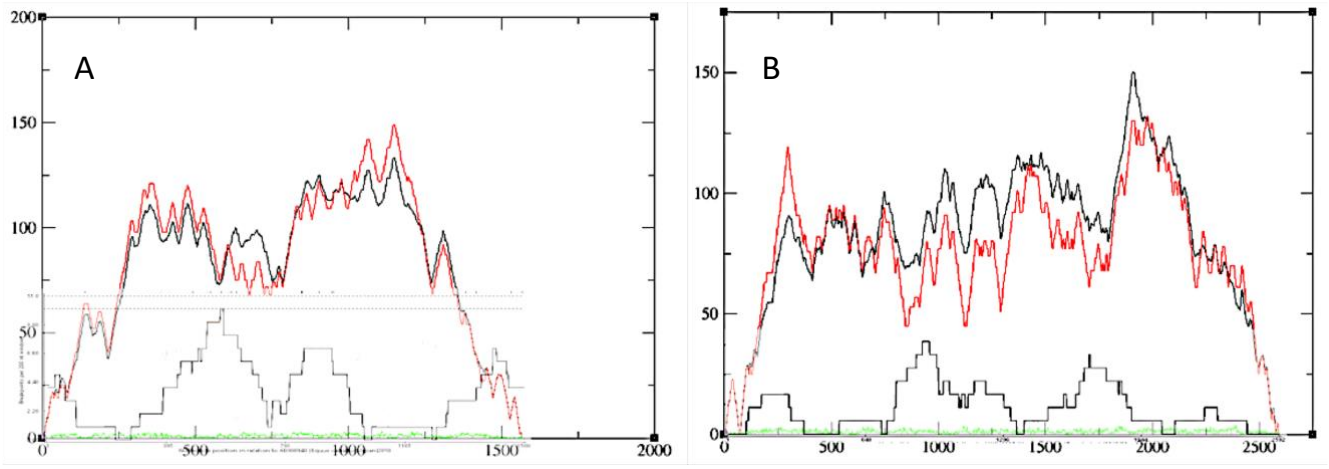

Supplementary Figure 2. *Consensus mountain plots of A) NSP1 and B) VP3 with recombination breakpoint distribution plot in gray.*